U.S.NRC
United States Nuclear Regulatory Commission
Protecting People and the Environment

NUREG/CR-7305

Metal Fuel Qualification

Fuel Assessment Using NRC NUREG-2246, "Fuel Qualification for Advanced Reactors"

Office of Nuclear Regulatory Research

AVAILABILITY OF REFERENCE MATERIALS IN NRC PUBLICATIONS

NRC Reference Material

As of November 1999, you may electronically access NUREG-series publications and other NRC records at the NRC's Library at www.nrc.gov/reading-rm.html. Publicly released records include, to name a few, NUREG-series publications; *Federal Register* notices; applicant, licensee, and vendor documents and correspondence; NRC correspondence and internal memoranda; bulletins and information notices; inspection and investigative reports; licensee event reports; and Commission papers and their attachments.

NRC publications in the NUREG series, NRC regulations, and Title 10, "Energy," in the *Code of Federal Regulations* may also be purchased from one of these two sources:

1. **The Superintendent of Documents**
   U.S. Government Publishing Office
   Washington, DC 20402-0001
   Internet: https://bookstore.gpo.gov/
   Telephone: (202) 512-1800
   Fax: (202) 512-2104

2. **The National Technical Information Service**
   5301 Shawnee Road
   Alexandria, VA 22312-0002
   Internet: https://www.ntis.gov/
   1-800-553-6847 or, locally, (703) 605-6000

A single copy of each NRC draft report for comment is available free, to the extent of supply, upon written request as follows:

Address: **U.S. Nuclear Regulatory Commission**
Office of Administration
Digital Communications and Administrative Services Branch
Washington, DC 20555-0001
E-mail: Reproduction.Resource@nrc.gov
Facsimile: (301) 415-2289

Some publications in the NUREG series that are posted at the NRC's Web site address www.nrc.gov/reading-rm/doc-collections/nuregs are updated periodically and may differ from the last printed version. Although references to material found on a Web site bear the date the material was accessed, the material available on the date cited may subsequently be removed from the site.

Non-NRC Reference Material

Documents available from public and special technical libraries include all open literature items, such as books, journal articles, transactions, *Federal Register* notices, Federal and State legislation, and congressional reports. Such documents as theses, dissertations, foreign reports and translations, and non-NRC conference proceedings may be purchased from their sponsoring organization.

Copies of industry codes and standards used in a substantive manner in the NRC regulatory process are maintained at—

The NRC Technical Library
Two White Flint North
11545 Rockville Pike
Rockville, MD 20852-2738

These standards are available in the library for reference use by the public. Codes and standards are usually copyrighted and may be purchased from the originating organization or, if they are American National Standards, from—

American National Standards Institute
11 West 42nd Street
New York, NY 10036-8002
Internet: www.ansi.org
(212) 642-4900

Legally binding regulatory requirements are stated only in laws; NRC regulations; licenses, including technical specifications; or orders, not in NUREG-series publications. The views expressed in contractor prepared publications in this series are not necessarily those of the NRC.

The NUREG series comprises (1) technical and administrative reports and books prepared by the staff (NUREG–XXXX) or agency contractors (NUREG/CR–XXXX), (2) proceedings of conferences (NUREG/CP–XXXX), (3) reports resulting from international agreements (NUREG/IA–XXXX),(4) brochures (NUREG/BR–XXXX), and (5) compilations of legal decisions and orders of the Commission and the Atomic and Safety Licensing Boards and of Directors' decisions under Section 2.206 of the NRC's regulations (NUREG-0750), (6) Knowledge Management prepared by NRC staff or agency contractors (NUREG/KM-XXXX).

U.S.NRC
United States Nuclear Regulatory Commission
Protecting People and the Environment

NUREG/CR-7305

Metal Fuel Qualification

Fuel Assessment Using NRC NUREG-2246, "Fuel Qualification for Advanced Reactors"

Manuscript Completed: April 2023
Date Published: August 2023

Prepared by:
W. Williams[1], C. Matthews[2], Y. Miao[3],
F. Di Lemma[1], L. Capriotti[1], Y. Wang[1],
C. Jensen[1], D. Keiser[1], C. Adkins[1],
D. Crawford[1], S. Novascone[1], D. Wachs[1]

[1]Idaho National Laboratory
Idaho Falls, ID 83415

[2]Los Alamos National Laboratory
Los Alamos, NM 87545

[3]Argonne National Laboratory
Argonne, IL 60439

James Corson, NRC Project Manager

Office of Nuclear Regulatory Research

ABSTRACT

Companies looking to license reactors with different materials than the current U.S. fleet of light-water zirconium-clad ceramic fuel are emerging as part of the push toward a more responsible energy economy. As such, the Nuclear Regulatory Commission is tasked with evaluating these new license applications. This report documents the current state of available experiment measurements, simulation capability, and historic knowledge and lessons learned required for evaluating sodium-cooled fast-spectrum metallic fuel, specifically U-10wt%Zr, up to 10at% burnup.

TABLE OF CONTENTS

LIST OF FIGURES

LIST OF TABLES

ACKNOWLEDGMENTS

This manuscript has been authored by Battelle Energy Alliance, LLC, under Contract No. DE-AC07-05ID14517 with the U.S. Department of Energy. The U.S. Government retains and the publisher, by accepting the article for publication, acknowledges that the U.S. Government retains a nonexclusive, paid-up, irrevocable, world-wide license to publish or reproduce the published form of this manuscript, or allow others to do so, for U.S. Government purposes. This research made use of the resources of the High-Performance Computing Center at Idaho National Laboratory, which is supported by the Office of Nuclear Energy of the U.S. Department of Energy and the Nuclear Science User Facilities under Contract No. DE-AC07-05ID14517.

The authors would also like to acknowledge technical editing and formatting contributions from Allie Madden, Publications Coordinator at Idaho National Laboratory.

ABBREVIATIONS AND ACRONYMS

AOO	anticipated operational occurrences
BDBA	beyond-design-basis accidents
BOL	beginning of life
BU	burnup
DBA	design-basis accident
FBTA	fuel behavior test apparatus
FCCI	fuel-cladding-chemical-interaction
FCMI	fuel-cladding-mechanical interaction
FFTF	Fast Flux Test Facility
FIPD	Fuel Irradiation and Physics Database
IFR	integral fast reactor
MFF	metal fuel in FFTF
MOOSE	Multiphysics Object-Oriented Simulation Environment
NRC	Nuclear Regulatory Commission
PIE	post-irradiation examinations
QA	quality assurance
SFR	sodium fast-cooled reactors
TREAT	Transient Reactor Test Facility
WPF	Whole Pin Furnace

1 INTRODUCTION

1.1 Purpose

This report is a generic response to NUREG-2246 “Fuel Qualification for Advanced Reactors” [1] for the uranium-zirconium (U-Zr) metal fuel system, informed by existing publicly available information, and assesses the future research potential for both accelerated fuel qualification and fuel qualification beyond the operating envelope described here. Fuel dimensions are included in this report; however, the implications of specific fuel design dimensions are best addressed with specific reactor designs, so metal fuel bulk phenomena and bounding conditions are the primary focus for this document. Additionally, this document may require revision or amendment to address specific fuel geometries or entire fuel bundles to adequately meet the needs of NUREG-2246.

The first task is to evaluate whether the objectives described in NUREG-2246, "Fuel Qualification for Advanced Reactors" (NRC 2021), are met for U-10Zr in HT9 cladding, the primary candidate fuel for future U.S. fast reactors [2, 3, 4, 5, 6], or whether there are gaps in the existing database. The assessment criteria, specific design parameters, material specifications, and operating envelope and design-basis operating conditions are laid out in Chapter 2. Chapter 3 presents test results, prior operating experience, and analyses to demonstrate with reasonable assurance that the specified fuel design is qualified for use under those conditions. Chapter 4 describes the modeling and simulation expertise garnered over the extensive history of U-Zr-based metallic fuel testing. Extending this case to design features or design-basis operation outside the scope of this document are possible through a technical case addressing the gaps or preparation of a separate document similar to this one that addresses the specific application and is addressed in Chapter 4.

The goal of fuel qualification is to:

1. Provide reasonable assurance that the specified fuel design will serve its design-basis functions under design-basis conditions, including design-basis accidents, in accordance with the reactor safety case.
2. Establish that the specified fuel design can be deployed in production using quality assurance and control typical of operating reactors, without additional quality control or fuel surveillance applied to new fuel designs with remaining fuel performance uncertainty.
3. Decouple the fuel system details from the overall reactor safety case by demonstrating that fuel life-limiting and safety-related phenomena are identified and sufficiently understood to ensure safety case assumptions about fuel behavior are valid.

As such, fuel qualification seeks to ensure safety criteria and practical objectives, such as fuel utilization, fuel reliability, and efficient reactor operation, are met by the fuel design.

1.2 Scope and Fuel Design Description

The scope of this fuel qualification assessment is defined by the fuel design and operating conditions, including selected safety-impacting limits. These are stated in this section along with a description of the fuel system. This initial qualification, while containing other conditions to be discussed, hereby extends to 10 at% burnup (BU). U-Zr system applications exceeding this BU limit will require additional monitoring, surveillance, and testing (particularly for transients off-normal behavior). Up to the 10 at% BU limit covered in the operational envelope discussion in Section 2.3 behavior of the U-Zr fuel system is well established and understood, see Section 3

and Section 4, and should not require continuous surveillance should the operational envelope be adhered to. While there are lifetime-limiting phenomena, they should not impact the fuel system to the point of requiring remediation or further understanding until deviating from the previously demonstrated operational bounds. These phenomena are discussed in the final sections to aid in fuel qualification outside of the bounds described here.

A brief review of the Experimental Breeder Reactor 2 (EBR-II) provides a good description of the history of metallic fuel development. During EBR-II's operation (1964–1994), it demonstrated metallic fuel as a viable option for fast reactors. EBR-II initial operation utilized U-fission fuel, or uranium alloyed with fission products that are difficult to remove during reprocessing.

Operating EBR-II as an irradiation facility motivated improvements in fuel utilization toward a higher discharge BU, and as a result, researchers identified metal fuel design principles to negate the fuel swelling and fission gas release behaviors that initially constrained fuel BU. As they gained experience on the impact of temperature and dose on the fuel and cladding, the core was transitioned to U-10Zr[1] metallic fuel, clad in a handful of materials (i.e., CW 316SS, CW D9, and HT9). In addition, they tested a wide swath of fuel parameters, including various concentrations of zirconium and plutonium. The collocation of EBR-II next to unique experimental facilities led to an extensive collection of irradiated pins and corresponding post-irradiation examinations (PIE), resulting in an unmatched database for understanding irradiated metallic fuel behavior.

To establish a starting point for evaluating metallic fuel fast reactor designs, the fuel design addressed herein is based on prior U.S. metal fuel experience with sodium-cooled fast reactors, specifically zirconium-based metallic fuel irradiated in EBR-II and the Fast Flux Test Facility (FFTF) [7,8,9]. The fuel rod is U-10Zr clad in HT9, with Na filling the initial fuel-cladding gap. The fuel rods are each spiral wound with an HT9 wire to ensure rod spacing when bundled into hexagonal arrays. Arrays have historically been 61 or 91 pins in EBR-II and 169 pins in FFTF. The fuel bundles are contained in a hexagonal duct (or "hex can"), which provides structural support and a defined coolant channel for each fuel assembly. Nominal values of definitive fuel design parameters are listed in Table 1-1. These design parameter values are derived directly from experience with metallic fuel test assemblies and qualification assemblies irradiated in FFTF. The design is considered the reference design for this qualification case. Approximate details are presented in Table 1-1 and Figure 1-1; requirements and tolerances are presented in later sections.

[1] Unless otherwise specified, all compositions are in weight percent.

Table 1-1 Fuel Rodlet and Assembly Parameters Similar to FFTF Series III.b Design

Parameter	Value
Nominal fuel composition U-10Zr	Nominal fuel composition U-10Zr
Fuel theoretical density 16.2 g/cm^3	Fuel theoretical density 16.2 g/cm^3
Fuel slug smeared density 75%	Fuel slug smeared density 75%
Plenum-to-fuel volume ratio 1.4	Plenum-to-fuel volume ratio 1.4
Fuel height 91 cm	Fuel height 91 cm
Fuel outer diameter, as-fabricated 0.5 cm	Fuel outer diameter, as-fabricated 0.5 cm
Fuel-cladding bond Na	Fuel-cladding bond Na
Cladding material HT9	Cladding material HT9
Cladding outer diameter 0.69 cm	Cladding outer diameter 0.69 cm
Cladding inner diameter 0.57 cm	Cladding inner diameter 0.57 cm
Wire wrap material HT9	Wire wrap material HT9

1.3 Limitations

As written, this metal fuel qualification assessment applies to the reference fuel design described in Section 2.1 within the operating conditions and constraints described in Section 2.3, which best match the U.S. experience base for this type of fuel. Extending this assessment to design variants and other operating conditions can be made by addressing the impact of departure from those design parameters and operating conditions on the fuel behaviors (fuel life-limiting and safety-affecting phenomena) described in Chapter 2. The suitability of the extended fuel qualification case should be confirmed through a fuel performance demonstration, typically using a monitored set of lead test assemblies to ensure that fuel behavior is as expected in the fuel qualification and reactor safety cases. These lead test assemblies should be among those that surpass other core assemblies in the feature being extended or changed (e.g., BU accumulation or exposure, power, temperature, or design) and should represent ranges of assembly performance. Even for the reference fuel design addressed herein, we recommend fuel behavior and performance be periodically monitored to establish fuel from a new manufacturing line being used in a new reactor exhibits the expected behavior up to the terminal peak BU value.

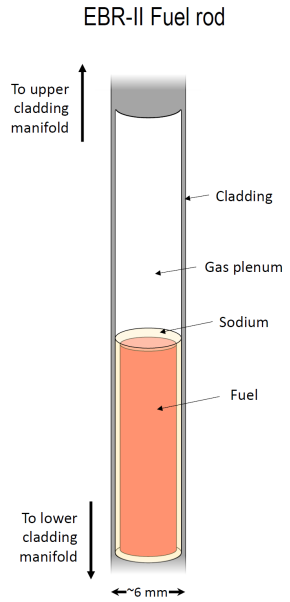

Figure 1-1 Sketch of a Typical EBR-II MK-IV Fuel Rod (Not to Scale), Adapted from [10]

2 METALLIC FUEL ASSESSMENT CRITERIA

This section defines the reference fuel design and operating conditions, details the safety case under these two umbrellas, and was generated through assessing prior fuel operating experience, fuel behaviors, and analysis to fulfill its design and safety functions for the reference operating conditions. Subsequent sections address the evaluation by experimental data and a fuel performance model, summarize the supporting database, and provides metal fuel source term characteristics. This document does not address a specific reactor design, so any subsequent application of this qualification case should address specific design-basis accident conditions and expected fuel responses.

At the highest level, the design-basis and safety functions that a fuel design must fulfill are specific to each reactor design. However, for sodium-cooled fast reactors, those functions can be stated generally as:

- Position fissile material in the reactor core stably and predictably for a controlled fission reaction.
- Allow the effective transfer of nuclear reaction heat from the fuel to the coolant (or heat transfer medium).
- Contain radionuclides (fuel and fission products) for operational convenience and a first safety barrier.
- Provide a convenient means of loading fresh fuel into the core and removing and managing spent fuel.

2.1 Fuel Design and Manufacturing Specification

In order to qualify metallic fuel as a driver fuel for the Integral Fast Reactor (IFR), researchers used the EBR-II and FFTF reactors (see Table 2-1 for general reactor specifications) to irradiate the reference IFR fuel, U-10Zr, via a series of metallic fuel tests. The most applicable to the dimensions and operating conditions proposed herein are the metal fuel in FFTF (MFF) experiments performed in FFTF and IFR tests performed in EBR-II. These tests used U-10Zr, clad in HT9 with a 75% smear density, and we will on them to build the safety case. Combined with the experience of U-10Zr fuel as a driver fuel for EBR-II [11], these efforts proved that the zirconium-based metallic fuel system was easily fabricated by injection casting [12]. Injection casting U-Zr fuel results in final-form geometry and requires no finishing steps (other than trimming to final length), making it highly repeatable, with master alloying and homogenization being unnecessary [12,13]. Over 35,000 metallic-based fuel elements were fabricated this way between 1964 and 1969, with over 100,000 injection castings (of various alloys). The history of the injection casting process has been outlined by Wilkes et al. [13].

Table 2-1 EBR-II and FFTF Reactor Parameters [14]

Parameter	EBR-II	FFTF
Power rating [MW]	62.5	400
Core volume [l]	1,040	1,040
Core height [m]	0.91	0.91
Core diameter [m]	1.21	1.21
Peak flux [10^{15} n/cm^2·s]	2.5	7.2
Average flux [10^{15} n/cm^2·s]	1.5	4.5
Peak linear power [kW/m]	27	42
Average linear power [kW/m]	23	24
Final driver fuel	U-10Zr	UO_2/PuO_2

The fuel design parameters and specifications addressed in this document are presented below. The supporting database of test results and operating experience include sufficient variants from these parameter specifications to provide reasonable confidence in the stability of in-tolerance deviations.

2.1.1 Dimensions

The design requirements presented herein are based on the historical EBR-II fuel, FFTF metal fuel, and projected Power Reactor Innovative Small Module fuel designs. Fuel irradiation tests in EBR-II and FFTF included many design parameters. For example, the pin column heights were 34 cm (13.5 in.) and 91.4 cm (36 in.) for EBR-II and FFTF, respectively. Prior U-10Zr fuel rod fuel diameter ranges included fuel slug diameters of 4.4 mm (0.173 in.) and 5.7 mm (0.225 in.) in EBR-II and 5 mm (0.197 in.) for FFTF; cladding outer diameters of 5.8 mm (0.230 in.) and 7.37 mm (0.290 in.) for EBR-II and 6.84 mm (0.270 in.) for FFTF; and cladding wall thicknesses of 0.38 mm (0.015 in.) and 0.41 mm (0.016 in.) for EBR-II and 0.56 mm (0.022 in.) for FFTF. The duct enclosing the fuel pins in the six MFF assemblies irradiated in FFTF was made of HT-9, because HT-9's low irradiation-induced swelling minimized core distortion [15]. The fuel column can consist of a number of fuel slugs, with a smaller number of slugs preferred for simplicity in fuel fabrication as casting longer slugs can be challenging. For example, the tolerances provided in Table 2-2 are extrapolated from historic EBR-II specifications [16], where multiple 34 cm fuel slugs were cast, and comparable values were used in the FFTF metal fuel irradiations ANL-IFR-(33, 43, 44, 71, and 72). These dimensions are not rigid design requirements, but rather examples of a fuel system. Although different tolerance values on key dimensions might be justified by a sensitivity analysis or new experience, a key parameter that must be adhered to is the maximum smear density (e.g., total cross sectional area in the cladding occupied by fuel) of 75% as exceeding this will significantly influence cladding strain and fuel column growth. Moreover, the fuel performance (swelling, fuel-cladding-chemical-interaction [FCCI], fuel-cladding-mechanical interaction [FCMI], etc...) covered in Sections 3 and 4 assume a 75% smear density.

Table 2-2 Dimensional Tolerances of the U-Zr Fuel System

Characteristic	Nominal	Tolerance
Fuel column height	91.4 cm	0.675 cm
Fuel column width	4.98 mm	0.09 mm
Column straightness	0.38 mm	N/A
Cladding thickness	0.457–0.56 mm	0.012 mm
Pin outer diameter	5.842–6.86 mm	0.013 mm

2.1.2 Constituents

The fuel composition and tolerances provided in Table 2-3 agree with historic EBR-II specifications [16]. Analytical chemistry for the IFR lead test assemblies show about an 0.10 wt% Zr fluctuation along the length of the Zr fuel pins [13], meaning these tolerances are not only achievable, but conservative.

Table 2-3 Composition Tolerances of the U-Zr Fuel System

Component	Nominal	Tolerance
Fuel	U-10wt%Zr	1.5% local, 1% average
Fuel impurities	<2,000 ppm total	Reported for C, Fe, N, O, Si, Y, Ta, Nb
HT9 cladding	ASTM A826/A826M-95	ASTM A826/A826M-95

The zirconium alloy feedstock in EBR-II driver fuel and experiments had a 99.9% minimum purity. Historically, element bond sodium did not exceed the maximum impurity levels provided in Table 2-4.

Table 2-4 Composition Tolerances of the Na Bond

Element	Tolerance
Ca	10
C	30
Cl	30
Li	5
K	1,000
O	100

2.1.3 End-State Attributes

The end-state attributes are process driven and specific to injection-cast fuel slugs. Other fabrication mechanisms will require a detailed comparison to their injection-cast counterparts.

2.1.3.1 Fuel

Per EBR-II process specifications [16] and FFTF fuel element fabrication requirements [17], the end-state attributes for the fuel are:

- Oxide formation should be restricted. Historically, fuel slug manufacturing and all operations on the fuel alloy conducted above 150◦C were done in a vacuum (pressure less than 200 microns, Hg) or in an argon or helium atmosphere with under 300 ppm of total impurities. Subsequent de-molding, cutting to length, and inspection could be performed in air at room temperature. If any fuel slugs were stored for 24 hours or more, it was either in a sealed or taped metal or plastic container (under 20 liters) or in a dry atmosphere with a dew point under -10◦C (which also limited any hydride formation). Similar practices and caution should be applied unless there is a justification for deviation.
- Fuel slugs are injection cast into fused silica (quartz) molds, which can have a light interior film of ZrO2 to reduce fuel slug adherence to the mold.
- The finished fuel slugs can contain internal defects such that the density remains between +0.3 and -0.5 g/cc.

2.1.3.2 Sodium Bonding

Per EBR-II process specifications [16] and FFTF fuel element fabrication requirements [17], the sodium bonding end-state attributes are:

- The sodium in the annulus between the fuel slug (smear density) and jacket should be void free to the extent that any gaseous pockets, shrinkage areas, or non-wetting of the jacket or fuel slug does not exceed 90° of the circumferential direction. No limit is placed on the axial length of such defects. This requirement stems from ensuring local coolability on reactor startup.
- The quantity of sodium in the plenum shall be justified or 2.54 cm above the fuel (i.e., limited to a height that ensures, for the given mass of sodium, any sodium displaced from the fuel-cladding gap does not leave a single void large enough to create an unacceptably hot spot in the fuel slug).
- The sodium in the annulus may be bonded (or wet) to the jacket and fuel slug under 540◦C, in order to reduce voids in the bond sodium and ensure intended contact between the sodium and fuel and cladding surfaces.

2.1.3.3 Cladding

Extensive irradiation testing has been performed on U-Zr fuels with HT9 cladding [18, 19, 11, 20]. Per EBR-II process specifications [16] and FFTF fuel element fabrication requirements [17]:

- The plenum-to-fuel ratio must provide a sufficient fuel plenum volume to accommodate released fission gas and maintain internal pressures that do not lead to unacceptable cladding creep strain. Acceptable ratios, therefore, vary with the intended terminal BU and cladding temperature.
- The end plug weld shall be free of cracks, undercuts, surface porosity and inclusions, and excessive surface oxidation. The weld shall have a 100% penetration of the jacket

wall to plug end weld joint and a minimum effective weld thickness (root-to-surface distance minus any porosity and inclusions) equal to or greater than 80% of the jacket wall thickness. The weld shall have a leak-tight seal.

2.2 Safety Criteria

Metallic alloy fuels were developed to support the U.S. sodium fast reactor program that aimed to establish the technology required to deploy commercial reactors. As such, the reactor demonstration programs conducted at EBR-II and FFTF were stepping stones toward that end. Although the operating environment of a commercial plant might deviate from those of the demonstration and test reactors, data from the demonstration and test reactors has been sufficient to identify life-limiting phenomena and determine most necessary limits for safe metal fuel operation. However, applying existing data to specific design-basis conditions, and design-basis accidents in particular, requires analysis and assessment. To enable this assessment, the EBR-II and FFTF operating conditions and their related design-basis accidents are the reference by which fuel design and safety criteria are evaluated and prioritized. Per NUREG-2246, “Fuel Qualification for Advanced Reactors” [1], fuel performance and safety criteria must be established to support the design and evaluation of reactor systems. These criteria can be generally divided into three categories: margins to design limits under normal operation and anticipated operational occurrences, margin to radionuclide release during design-basis accident conditions, and ability to ensure a safe shutdown under all conditions. The relevant fuel design and safety criteria for each category is discussed in the following sections.

2.2.1 Design Limits During Normal Operation and Anticipated Operational Occurrences

Based on operating experience with metal fuel in EBR-II, the fuel design and safety functions are met if the fuel design ensures the following fuel performance requirements are met:

- Restrict the number of expected fuel-cladding breaches to a small number to maintain a low and manageable coolant radionuclide inventory; for a sodium-cooled fast reactor, this limit is usually one or fewer fuel rod failures per core load. A core load is expected to be approximately 12,000–16,000 fuel rods, based on experience with the FFTF Series I, II and III.b driver fuel designs. This is not a fuel safety limit, but a design objective to drive the margin against breach susceptibility due to in-service fuel degradation.
- Ensure that no fuel melting occurs, which prevents positive reactivity insertions due to fuel slumping and reduces cladding penetration by accelerated fuel-cladding interdiffusion. Ensure that dimensional changes resulting from creep (thermal or irradiation induced) and void swelling do not create unacceptable dimensional or shape changes in fuel components, which could otherwise impede coolant flow through fuel assemblies or control rod motion.

These design-basis operating conditions are used to populate the fuel performance envelope, presented in Section 2.3 . Applicants using this fuel would need to demonstrate that their core would be operated under the conditions supported by the available experimental database or otherwise address gaps through analysis and testing.

Historic irradiations immediately relevant to this design are listed in Table 2-5. EBR-II X425 was a lead IFR concept experiment. EBR-II X429 was an experiment designed to investigate fabrication variables. EBR-II X430 was a large-diameter fuel test experiment. EBR-II X431 and X432 were HT9-clad blanket fuel elements. The X447 test was inner blanket and driver type subassemblies containing 49 IFR fuel elements, 19 HT9-clad, and 30 D9-clad, along with 12

dummy (unfueled) elements. EBR-II X448–X451 were EBR-II Mark IV HT-9-clad fuel qualification tests. EBR-II X496 was an IFR experiment to demonstrate the high BU potential of metallic fuel. Subassembly X496, a 37-rod assembly design (with larger-diameter fuel rods), utilized the MK-D37A core type subassembly hardware with a 316SS hex duct and 37 U-10Zr enriched to 93% U-235 in 40-inch-long jackets. The listed FFTF irradiation experiments were part of the MFF series, which used HT9-clad U-10Zr in HT9 subassembly hardware. These tests were the first in an incomplete, larger campaign to qualify the Series III.b driver fuel design for FFTF.

Table 2-5 List of U-10Zr and HT9 Irradiation Experiments for Metallic Fuels [8]

Test ID	Pins	Peak Power [kW/m]	Peak Cladding Temperature [°C]	Peak Burnup [at. %]	Fast Fluence [10^{22} n/cm^2]	Comments
EBR-II-X425	34	48.2	590	19.3	20.6	
EBR-II-X429	12	42.7	600	14.4	13.8	Two breaches
EBR-II-X430	28	49.2	540	11.5	20.6	
EBR-II-X431	8	39.4	507	3.9	15.4	
EBR-II-X432	7	39.4	507	4.5	16.6	
EBR-II-X447	23	36.1	660	10	9.17	Two breaches
EBR-II-X448	68	45.9	552	14.6	14.9	
EBR-II-X449	61	29.5	578	11.3	17.7	
EBR-II-X450	61	36.1	576	10.2	13.2	
EBR-II-X451	65	32.8	623	13.7	13.7	
EBR-II-X496	37	63.3	536	8.3	6.9	
FFTF-MFF1A	8	42.7	577	3.8	5.6	
FFTF-MFF-1	5	43.0	577	9.5	17.3	
FFTF-MFF-2	169	54.1	618	14.3	19.9	
FFTF-MFF-3	169	59.1	643	13.8	19.2	
FFTF-MFF-4	169	56.8	618	13.5	19	
FFTF-MFF-5	169	55.8	651	10.1	14	
FFTF-MFF-6	169	55.8	588	14.1	12.8	

Under these tests and conditions, as detailed in later sections of this report, fuel and cladding dimensional changes were acceptable and did not impact fuel longevity up to 10 at% BU. Fuel melting, aside from FCCI, is also not achievable under the designated operating envelope or expected transients. However, the EBR-II X447 test, with two cladding breaches, best indicates

that, for higher cladding temperatures, the prevailing failure mechanism is stress rupture in cladding thinned by FCCI. Data from the MFF-3 and MFF-5 assemblies irradiated well beyond the proposed BU limit of 10 at% are most comparable to the breached pins and suggest that FCCI can be mitigated with lower inner cladding temperatures (which should be restricted to below 650°C for proper accommodation, including during anticipated operational occurrences [AOOs])—note that lower temperatures mitigate FCCI at any BU, though whether they mitigate enough depends on the situation. Within this temperature limit, the following sections show these operating conditions are well represented by successful historical irradiations. The test envelope outlines these conditions, and subsequent sections provide evidence and support that fuel performs within the envelope.

2.2.2 Design Limits During Anticipated and Accident Transients

The inherent thermal and neutronic performance of metallic fuel during transients or other off-normal conditions is an appealing feature that has been evaluated through multiple experimental approaches corresponding with specific conditions of interest. Reactor transients are commonly classified by the probability of occurrence including AOOs and accidents, also of differing likelihoods of occurrence. AOO events are characterized as those likely to occur at least once in the life of a reactor. These events include plant upsets, turbine trips, and loss of offsite power, including those where the plant protection system would respond. Local faults, such as a minor cladding breach, also belong in this category. Accidents are those that are not expected to occur during the life of the reactor and may be further split into unlikely to extremely unlikely events or probabilities of 10^{-2} to 10^{-4} and 10^{-4} to 10^{-6}, respectively. Typical unlikely accidents (considered design-basis accidents or DBAs because they are to be explicitly addressed in the reactor's design-basis) include single fault events, such as loss of coolant pumps with a reactor scram through the plant protection system. Extremely unlikely accidents (considered beyond-design-basis accidents, or BDBAs) include double fault events, such as a loss of coolant flow combined with a failure to scram the reactor. In sodium fast-cooled reactors (SFR), the most challenging events in the BDBA category tend to be anticipated transient without scram events. Even lower-probability severe accidents require the failure of three or major systems.

The inherent characteristics of metallic fuel support passive safety approaches in SFR designs. Key thermo-chemical-mechanical characteristics include a high thermal conductivity, relatively high fuel-to-cladding ductility ratio, chemical compatibility with the sodium coolant, and fuel liquidus temperatures close to the sodium coolant boiling point. For 75% fuel smeared density designs (higher fuel smeared densities will lead to a higher FCMI cladding strain), the primary fuel damage mechanisms (including fuel breach) in metallic fuels of various compositions in off-normal conditions are:

- Low-melting-point eutectics between the fuel and cladding, which can cause additional cladding wastage, distinct from the steady-state FCCI caused by lanthanide fission product cladding attacks. In nearly all cases, near-abrupt failure occurs when a fuel-cladding interface (direct contact) reaches 1080◦C.
- Cladding overpressure due to the high-temperature pressurization of accumulated fission gas in the fuel pin. From these mechanisms, corresponding design criteria ensure adequate margin to fuel damage.

The following design criteria correspond to these two degradation modes:

- Fuel melting should be precluded by plant design for normal operations, AOOs, and DBAs. This limit is primarily recommended due to the uncertainty in a comprehensive

predictive capability to define resulting behaviors such as fuel relocation and reactivity effects. Experiments have shown metallic fuel melting in EBR-II and the Transient Reactor Test Facility (TREAT) with no to little effect on the cladding integrity. In this context, fuel melting does not include forming low-melting eutectics from fuel constituents and fission products but does include the effects of fuel alloy redistribution.

- The as-mentioned 650◦C limit for the cladding and fuel-cladding interface (the fuel centerline can go to higher temperatures) applies to normal operations and should be adhered to in the FCCI region to prevent eutectic melting.
- During AOOs and DBAs, the cumulative eutectic penetrations should be maintained below a specified limit accounting for its effects as wastage. Although the application of cladding strain and cumulative damage fraction limits implicitly incorporates cladding thinning (cladding wastage) effects due to eutectic formation, the basis for limiting eutectic penetration is to limit (conservatively) the amount of liquid fuel phase. EBR-II requirements limited eutectic penetration to 5% of the cladding thickness, primarily to limit the formation of liquid fuel to under 10% based on Fuel Behavior Test Apparatus (FBTA) test data showing no propensity for fuel relocation at these levels.
- Core coolability is maintained in all conditions including BDBAs. Coolability is ensured by requiring no cladding melting, which can be indicative of sufficient melting and reformation to impede coolant channels. This requirement was met in EBR-II (and part of the design for the Clinch River Breeder Reactor) by preventing coolant from exceeding its boiling point. Any potential fuel failure requires a justification of limited fuel dispersal from the cladding, which may be based on experimental evidence of cladding failure characteristics.

Due to relatively high thermal diffusivity, cladding failure during transients has typically been characterized as occurring at the top of the fuel column where fuel-cladding interface temperatures are highest during normal operations and postulated transients. Fuel failure is typically preceded by significant axial expansion of the fuel driven by thermal expansion and fission gas coalescence and expansion. Upon reaching fuel melting, or temperatures at which the fuel is very soft, the molten fuel extrudes into the plenum region of the pin. Transient performance has been investigated on several fuel compositions. A brief description of testing and discovery is provided in this section as it supports utilizing accumulated experimental data from various fuel designs in justifying the performance of a particular specific fuel design. While varying levels of data exist to support different fuel designs, U-xPu-yZr fuels have similar performances because of similar fission gas release and fuel swelling characteristics, similar mechanical properties, and similar cladding-fuel eutectic temperatures dominated by the U-Fe interaction. Thermal limits generally vary somewhat between different alloy compositions, driving some distinctions in quantitative thresholds.

2.3 Fuel Performance Envelope

The steady-state operating envelope is based on experience with metal fuel in EBR-II and FFTF. These operating conditions, and the safety-impacting limits that follow, are considered herein as the reference deployment or high-level operating envelope for this qualification case. The limits for fuel operation and utilization include:

- Peak fuel rod BU of 10 at%: This limit, defined as the peak localized BU attained in any fuel rod, ensures that the combined effects of all fuel degradation mechanisms and performance phenomena do not lead to fuel breach rates that exceed the fuel-cladding breach rate requirement. Based on irradiation experience, the EBR-II Mark-III and Mark-

IIIA driver fuel, either D9 or 316SS clad U-10Zr fuel with similar smeared density and plenum-to-fuel ratio, were qualified for a BU limit of 10 at% [11].

- Peak linear heat generation rate at the beginning of life (BOL) of 40–55 kW/m: This limit is where, with a margin of error, extensive testing has been performed and associated fuel evolution kinetics are well characterized and acceptable.
- Peak 650◦C fuel-cladding-interface temperature for steady-state operation: This limit minimizes thermal creep of the HT-9 cladding and FCCI and prevents fuel-cladding liquefaction (i.e., formation of lower-melting-temperature phases in fuel-cladding interdiffusion zones and fuel-clad eutectic at 1080◦C). This limits the extent of FCCI to prevent significant cladding thinning that would make breach by stress rupture more likely and helps ensure that the fuel-cladding breach rate requirement is met. Often, this translates to a peak 620◦C outer cladding temperature; however, this will be influenced by cladding thickness and core design.
- Total radial strain and deformation of 2%: Alternatively, a limiting value of cumulative damage fraction could be applied or sources of strain be limited individually (e.g., cladding radial deformation from thermal creep remains 1%). The cumulative damage fraction is calculated from the known cladding stress rupture behavior and a statistical assessment of cladding failure probability that achieves a failure rate of no more than one failure in a core load of fuel rods. Cladding strain and damage fraction are measures of in-service cladding degradation, and these limits help ensure that the fuel breach rate requirement is met and that cladding deformation does not appreciably impede coolant flow or control rod motion. Beyond 10 at%, FCMI will contribute significantly to cladding strain and should be the primary feature surveyed.
- Peak fuel temperature: The fuel temperature is to remain below the local fuel composition solidus temperatures. This fuel temperature limit ensures that no fuel melting occurs that might lead to fuel slumping or accelerated fuel-cladding interdiffusion.

2.3.1 Behaviors, Phenomena, and Properties

Under the design limits and operational envelope for normal operation and AOOs, the following are the behaviors, phenomena, and properties of metallic fuel that impact fuel reliability, utilization, and safety:

- Geometric evolution:
    - Fuel swelling, which can place mechanical stresses on the cladding or impact core reactivity or coolability;
    - Cladding creep behavior, which is a key contributor to fuel rod deformation and the accrual of cladding damage potentially leading to stress rupture;
    - Cladding void swelling behavior (only a concern for 316SS and D9, not HT9 below 10 at% Bu), which is a key contributor to fuel rod deformation, cladding embrittlement, and the accrual of cladding damage leading to stress rupture.
- Fuel constituent migration, which establishes localized fuel composition deviating from bulk composition and thereby time- and location-dependent fuel solidus temperature;
- Fuel properties:
    - Solidus temperature, which is a key input into established fuel temperature limits;
    - Thermal diffusivity or conductivity, which is a determiner of fuel steady-state temperatures and transient responses;
    - Thermal capacity, which is a determiner of fuel steady (long duration) transient response.
- Cladding integrity and barrier degradation:

    - Yield stress;
    - Solidus temperature;
    - Thermal diffusivity or conductivity;
    - Thermal capacity;
    - Irradiation creep;
    - Embrittlement.
- Radionuclide release limits and retention requirement:
    - Cladding rupture criteria (due to fission gas release, overpressure, and FCCI cladding degradation);
    - Radionuclide retention, transport, and release;
- Fuel and cladding interdiffusion (or FCCI), which effectively thins the load-bearing portion of the cladding and leads to the formation lower-melting-temperature phases in the fuel and cladding;

This list is all inclusive for metal fuel designs used or investigated to date in the U.S. and is consistent with metal fuel experience reported internationally. In other words, these phenomena and properties determine or impact metal fuel safety, behavior, and utilization across all known fuel compositions (such as U-10Mo, U-Fs, U-Zr, and U-Pu-Zr), fuel designs (e.g., for varied fuel smeared densities and plenum-to-fuel volume ratios), and fuel deployment conditions. The impact of any phenomenon or property can vary by composition, fuel design parameters, and design-basis conditions, but if these behaviors can be established with reasonable confidence for a given fuel design and reactor design, the fuel can be qualified (i.e., demonstrated to fulfill its safety functions and design-basis functions for design-basis conditions). Section 3 details the experimental data, and Section 4 details the models that justify the safety case for the described operational envelope.

3 EXPERIMENT DATA UNDER FUEL PERFORMANCE ENVELOPE

This chapter discusses how the fuel evolves under the operating envelope, particularly with respect to fuel swelling, fission gas transport, and cladding degradation (including by FCCI and FCMI because radiation effects such as embrittlement or void swelling [in austenitics] also degrade cladding). The experiment data and PIE results, as well as models, in this report demonstrate how the aforementioned fuel assessment criteria are met.

3.1 Geometric Evolution

Metallic fuel undergoes severe geometric changes throughout irradiation. The most pertinent contribution to geometric evolution is fuel swelling. In U-10Zr, clad in HT9, in HT9 ducting, swelling has a minimal impact in the total cladding strain up to 10 at% BU and is not a safety concern in 75% smear density fuels. However, fuel swelling is discussed here to illustrate the acceptable behavior of this fuel system under the described operating envelope. Fuel swelling takes place in three dimensions, but due to cladding constraint, swelling can be simplified to axial and transverse swelling, (i.e., fuel column growth and radial strain, respectively).

Metallic fuel undergoes severe geometric changes throughout irradiation. Within the first couple at% of BU, the fuel swells—primarily due to the accumulation of insoluble gaseous fission products into large bubbles and solid fission product accumulation—and fills the free area provided by the fuel-cladding gap to come in contact with the cladding. A large, sodium-filled gap to accommodate fuel radial swelling was proven through testing in EBR-II to reduce FCMI and associated cladding strain [21], and this design feature is now standard in metal fuel designs for fast reactors. As the driving force for the extensive swelling is the large fission gas bubbles trapped in the fuel, swelling decreases rapidly once the gas porosity becomes interconnected. At this point, a pathway is provided for the fission gas to escape to the plenum instead of increasing bubble volume [22]. Under the thermal and power conditions outlined in the operational envelope presented in Section 2.3 , this interconnection occurs at approximately 1–2 at% BU [23]. After the fuel-cladding contact is established, cladding friction inhibits axial elongation [24]. This is supported by various PIE results [25, 26, 27, 28]. Subsequent swelling due to solid fission product buildup is accommodated by plastic deformation of the highly porous fuel constrained by the cladding up to about 10 at% BU. For eventual fuel qualification beyond 10 at%, the fuel swelling and solid fission products may reduce the interconnectivity and a second rapid spike in swelling may occur. However, this is not a concern below 10 at% BU.

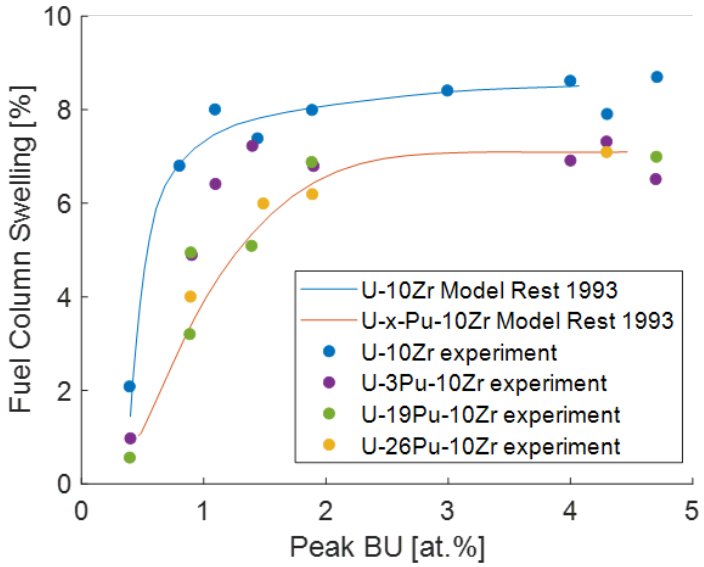

Figure 3-1 Axial Fuel Swelling of U-xPu-10Zr Alloy Fuel [23,24]

Figure 3-1 illustrates fuel column swelling (i.e., fuel column axial elongation) as described by modeling and experimental data [24, 23, 29]. During these early stages of normal operation, swelling occurs anisotropically with the majority occurring as radial growth until contacting the cladding and the initial smear density is consumed [24, 23, 29, 30]. Fuel elongation can vary drastically as a function of smear density as the eventual cladding contact induces sheer stresses that impede axial expansion and growth [24]. A smear density of 75% allows for approximately 30–33% total volumetric fuel swelling prior to fuel-cladding contact and typically results in an 8–9% fuel column elongation [31, 24, 23, 29, 32]. This 75% smear density is still commonly used as 30% fuel swelling is approximately when fission gas porosity becomes interconnected, allowing for a gas release to the plenum and sharply slowing the swelling rate [33]. Lower smear densities typically result in greater anisotropic swelling.

Although simple, this swelling description conservatively captures the key impacts for fuels up to 10 at% BU. While only select fuel pins were used to generate Hofman and Rest's models [24, 23], it can be readily observed to pertain to a plethora of U-10Zr fuels, whose growths were extracted from Fuel Irradiation and Physics Database (FIPD) radiography data [34], as shown in Figure 3-2. Again, exceeding 10 at% BU will eventually constrain the porosity network, eliminate the path to the plenum, and cause a second spike in fuel swelling. This process is not yet fully understood mechanistically and should be a primary feature of future fuel surveillance programs as BUs increase beyond the 10% threshold proposed here.

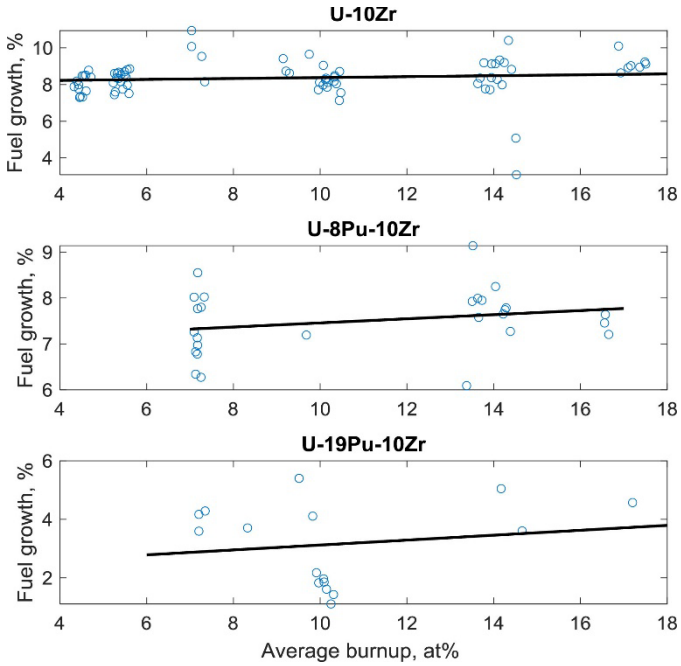

Figure 3-2 Average Percent of Axial Fuel Growth as a Function of BU for Three Different Fuel Compositions, Extracted from the FIPD Database [34]

Figure 3-3 contains a subset of the relevant FIPD data for U-10Zr fuel pins clad in HT9 with an initial 0.439-cm-diameter slug. Additional relevant fuel pins are available in the FIPD database; however, these preliminary results are adequate for discussion. This discussion includes axial growth tending to first increase with BU due to fuel swelling and then retract above 5 at% BU. This is hypothesized to be due to fuel creep and fuel slug “slumping” during irradiation and, while relatively expected [3, 35, 36], provides further insight on the slumping occurring as a function of fuel centerline temperature. While there is currently a perceived data gap between 5 and 10 at% BU, this is due to the nature of the plot being against peak values. For localized measurements, the best study was conducted by Paaren et al. [37]. Additional effort will be able to capture local behavior and adequately cover the operation envelope. Axial growth and cladding strain also tend to show an increasing correlation with temperature, something that is not captured in historic empirical comparisons to only BU. Local fuel swelling measurements compared to models can be readily found in literature [37]

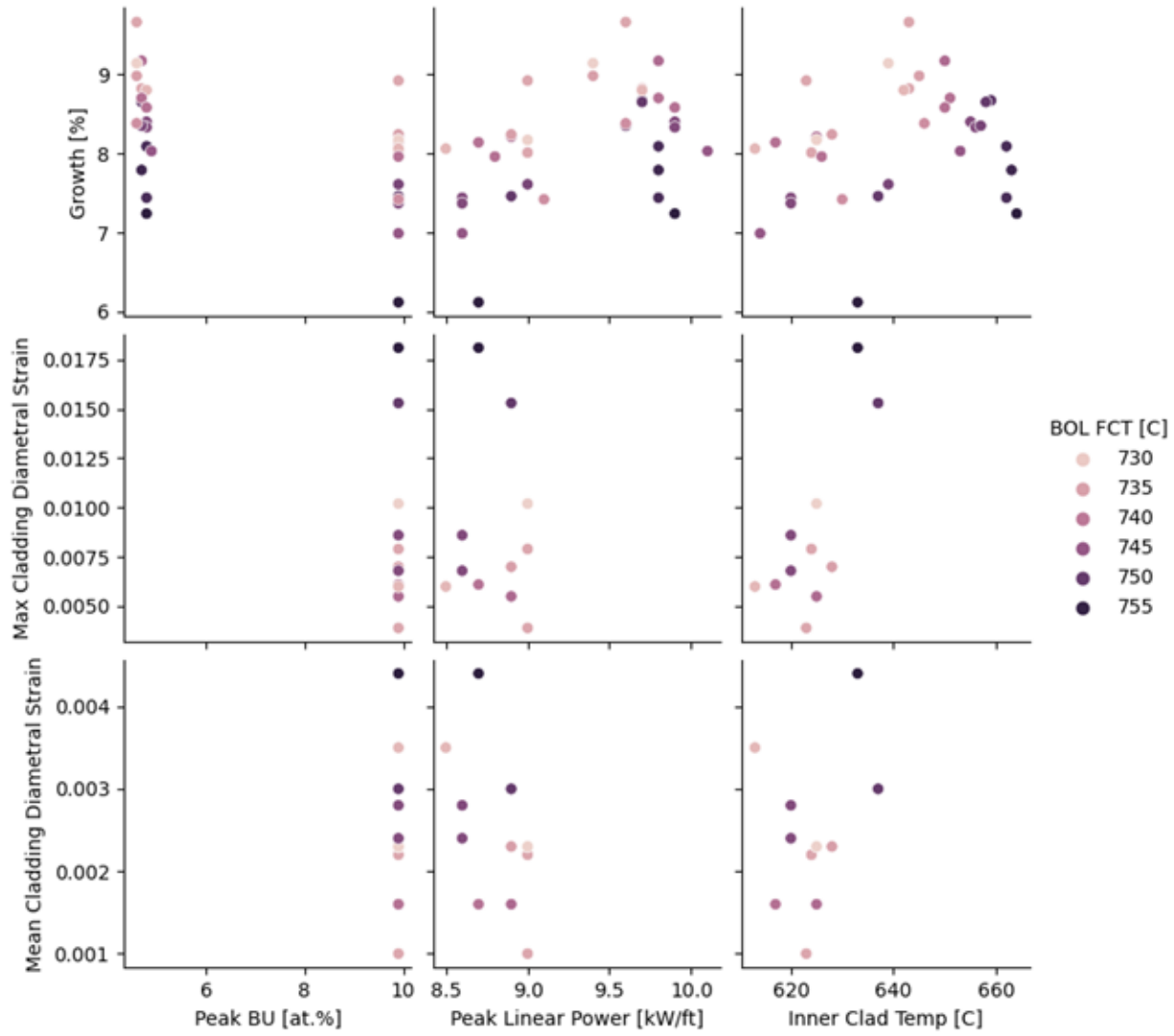

Figure 3-3 Pair Plot of Growth and Strain Metrics Versus Peak BU, Linear Power, and Inner Clad Temperature Color Coded to Fuel Centerline Temperature for U-10Zr Fuel Pins with a Typical Slug Diameter of ~.439 cm [38]

The recent studies [10, 39, 20] show that fuel swelling is well understood and can be reliably modeled. This modeling effort is discussed in Chapter 4. Regardless, the experimental and empirical data alone suggests that cladding strain should not exceed 2% and is not a limiting factor with respect to fuel longevity under this operating envelope. This 2% value includes thermal creep, swelling-induced cladding strain, and FCMI as only final cladding strain can be measured. Any models used in lieu of empirical cladding strain data must not be limited to a single feature such as swelling or thermal creep. During the eventual increase of the BU limit (from 10 at%), swelling should be further investigated to ensure cladding is not overly strained by the eventual closing of the interconnected porosity network due to solid fission product accumulation.

3.2 Fuel Constituent Migration

In U-Zr-based (binary and ternary) fast reactor fuel systems, there is an elemental redistribution, or de-mixing, of U and Zr. This phenomenon, termed constituent redistribution, is primarily driven by the thermal gradient within the fuel [40, 41, 42]. The thermal gradient exists due to the large amount of energy imparted on the fuel system during fission in a self-insulating geometry (cylinder). This gradient extends from the peak value at the self-insulated fuel center to the thermal sink at the fuel-cladding interface. As fission occurs in the fuel, fission gases form porosity, decreasing thermal conductivity throughout irradiation and increasing the thermal gradient, and subsequent de-mixing, further [43, 44]. Qualitatively, the zirconium moves from the mid-temperature β-U phase to the high-temperature γ-U phase, resulting in a ring-like structure with 30 wt% Zr in the center region, 5 wt% in the mid-temperature region, and the as-fabricated concentration of U-10 wt% in the outer rim of the slug [28]. This redistribution is likely accelerated by irradiation, where vacancies and vacancy flux can influence constituent diffusion at least as much as chemical potentials [45]. In irradiated material, the size and number of distinctly redistributed zones (2–5) varies with irradiation conditions, initial fuel composition, and initial fuel geometry. It is immediately apparent that the large compositional inhomogeneity following redistribution will result in different phase concentrations, phase morphology, thermophysical properties, and grain sizes.

These changes can affect properties, including thermal conductivity, local power density, diffusivity, solidus temperature, and sink density. However, these nuances are not of concern prior to 10 at% BU as the impact of redistribution is already accounted for in all PIE data and a Zr-depleted region is assumed (e.g., regardless of the linear heat generation rate and thermal gradient, the end result is a Zr-depleted region and FCCI that is accounted for). Moreover, the redistribution occurs in a favorable directions, with Zr migrating towards the hotter central region, lowering the local power and increasing the solidus temperature, negating the change in the thermal conductivity (i.e., the regions with increased power are nearer heat sinks). As fuel is irradiated beyond this prescribed operating envelope, redistribution may become a larger metric for fuel performance, but, at this time, the fuel-cladding eutectic temperature is below the solidus temperature even in the Zr-lean regions. Chapter 4 discusses the fuel system modeling, and while accurate, does not account for redistribution.

3.3 Fuel Properties

Various phase diagrams (e.g., [46, 47, 48]) illustrate that the lowest solidus temperature of the U-Zr system is greater than 1100◦C. This means that, with respect to fuel properties and solidus temperature, the operating limit is nearly double the proposed operating temperatures. This does not hold for the FCCI region (fuel-clad eutectic) and is discussed in Section 3.4 . Bulk fuel melting is not a concern under this operating envelope.

There is little experimental data available on thermal conductivity and diffusivity, which are discussed in more depth in the modeling sections in Chapter 4. However, metallic fuels are highly conductive when compared to their UO2 counterparts as shown in Figure 3-4. Owing to the large thermal conductivity of metallic fuel, there are no indications of thermal conductivity diminishing to the point of concern during irradiation, even when considering the high amount of porosity present in the fuel. There are, however, multiple studies and models that can illustrate that thermal conductivity sufficiently retains coolability as a function of BU while accounting for porosity and redistribution [49, 43, 44, 50, 51].

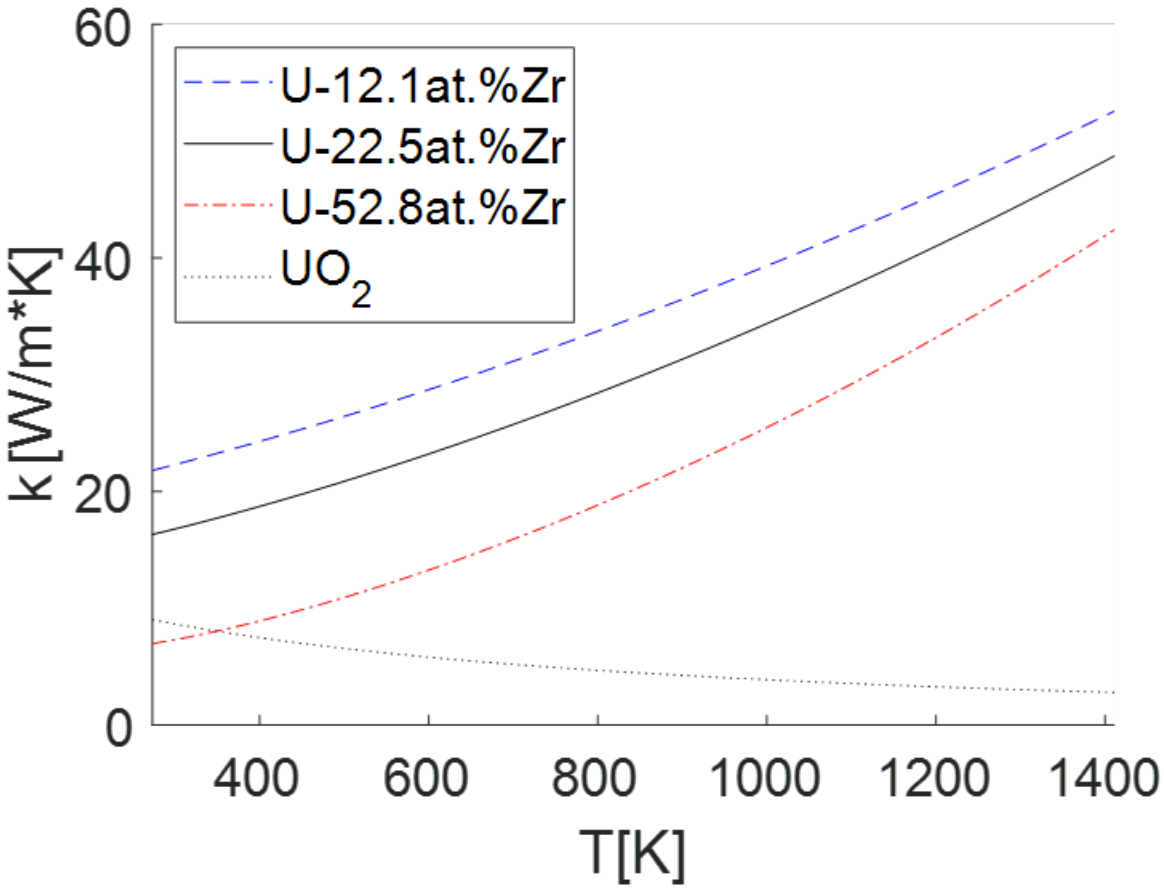

Figure 3-4 Thermal Conductivity of Unirradiated U-X at% Zr for X = 12.1, 22.5, and 52.8, Corresponding to 6, 10, and 30 wt%, Respectively, (Following Galloway's Model [26]) and UO2 (Following Fink-Lucuta's Model [52]) as Obtained from the BISON Theory Manual [53]

The effect of porosity on thermal conductivity is described in the BISON model by

$$k = k_0 * \frac{1-P}{(1+\beta P)} \tag{3.1}$$

where P is the porosity volume fraction and β is an empirical factor typically set to 2.5 [53]. The porosity effect on thermal conductivity is illustrated in Figure 3-5, showing the need to accurately predict porosity development and subsequent fuel swelling as thermal conductivity will vary substantially as a function of porosity, albeit while retaining thermal conductivity an order of magnitude higher than UO2 without factoring in Na logging, which will further increase thermal conductivity.

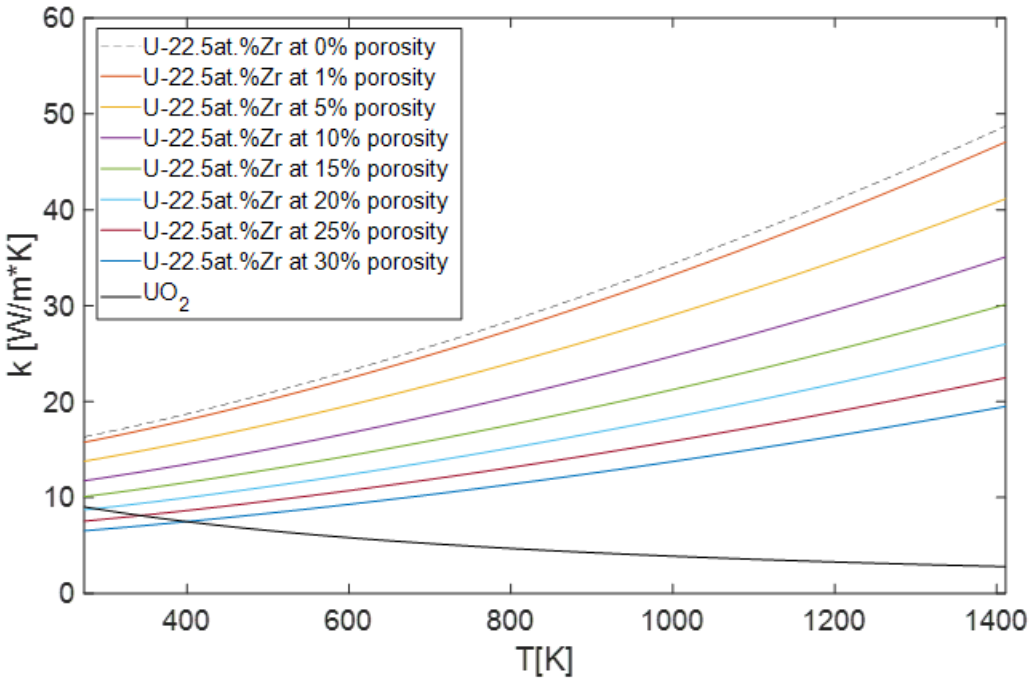

Figure 3-5 Illustration of Porosity, Ranging from 0 to 30%, Influencing Thermal Conductivity in the U-Zr System as Obtained from the BISON Theory Manual (Note: U-22.5at.%Zr is U-10wt.%Zr)

3.4 Cladding Integrity and Barrier Degradation

Fuel cladding, the boundary between the metallic fuel and coolant, is the most critical barrier to prevent the release of fission products into the coolant (and minor, but possibly present, mechanical corrosion of fuel by the coolant). Therefore, phenomena that can cause cladding degradation or failure under normal operation and off-normal (accident) conditions must be properly understood and factored into reactor fuel safety designs. These phenomena can be described as cladding integrity and degradation.

Cladding integrity essentially equates to FCMI. FCMI was one of the first historic problems to be addressed in this system. The FCMI onset was mitigated by reducing the smear densities to accommodate the inevitable swelling. It is important to note that these design features do not limit fuel swelling. Rather, they allow the fuel to swell to the point of fission gas porosity interconnectivity, where fuel swelling decreases sharply due to direct fission gas release to the plenum. With a properly designed fuel plenum and smear density, cladding strain is minimized [4], and yield strength is not a concern. Thus, FCMI is not a life-limiting phenomena during normal operation up to 10 at% BU [54]. However, it should continuously be recalled as higher BUs are achieved due to the inevitability of solid fission product buildup that can constrain the fission gas pathways and cause secondary volumetric instability or rapid growth.

Driver fuel behavior under off-normal conditions (loss of cooling, transient overpower) has demonstrated that cladding breach will not occur, including a series of loss-of-cooling tests. Mark-IIIA and Mark-IV driver fuel, after irradiation to 9 at% BU, could survive a 0.1%/s overpower transient to 40% overpower without a cladding breach [11]. Moreover, out of all the

HT9-clad U-10Zr fuel pins irradiated with a 75% smear density, none have breached due to cladding strain. HT9 cladding also significantly outperforms the 20% cold-worked 316SS cladding in both strength and ductility between 370 and 615◦C [55]. Indications of minor irradiation hardening at high stress and softening at failure temperatures above 700◦C were observed, but these remain outside of the proposed operating envelope [55]. It has also been shown that HT9-clad metallic fuel elements have reached 17.5 at% BU without a cladding breach [56]. A comparison of cladding diametrical strain as a function of cladding is shown in Figure 3-6.

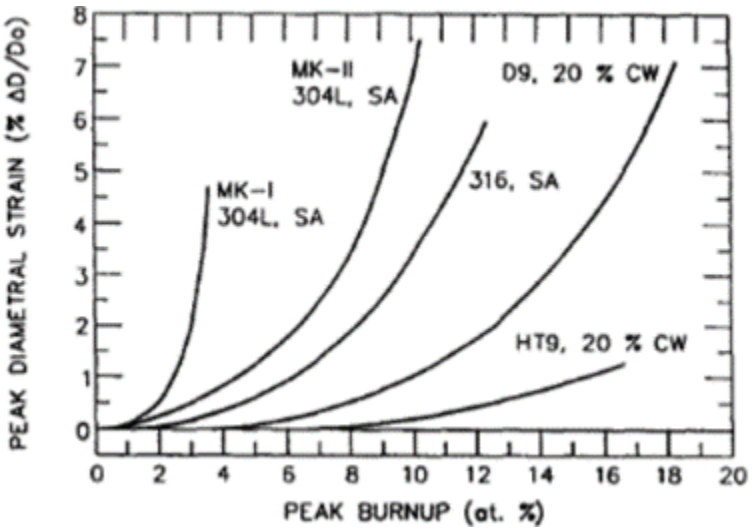

Figure 3-6 Progressive Improvement in the Deformation (Swelling and Creep) of the Cladding of Metallic Fuel Elements in EBR-II Irradiations, where SA: Solution Annealed and CW: Cold-Worked [56]

Due to the creep behavior of metallic fuel and the swelling accommodation via smear density, HT9 yield stress and ductility is not a direct concern. Beyond 10 at% BU, the accumulation of gaseous fission products in the fuel pin plenum may eventually lead to the ballooning of otherwise-intact cladding. Perhaps the only concerning factor below 10 at% BU is FCCI, which if irradiation occurs at high temperatures, may embrittle the cladding and lower the solidus temperature of the fuel. FCCI is the primary failure mode for U-10Zr fuels (which may lead to cracking and cladding breach) and has been identified as the primary source for cladding degradation and the most limiting failure mode under overpower or transient conditions [57, 58]. While the temperature limits proposed in this operating envelope are below the solidus temperature of the interaction zone as well as below the temperature that drastically accelerates FCCI, the only HT9-clad U-10Zr fuel pins failures were due to FCCI, warranting further discussion.

FCCI is a result of chemical interdiffusion between the fuel and cladding constituents when the metal fuel contacts the cladding, which is driven by fuel swelling. The primary example of this is the formation of a U/Fe eutectic due to constituent interdiffusion. This interdiffusion is accelerated due to the presence of lanthanide fission products. Previous irradiation and PIE on fuel-cladding interaction has gained some understanding of the interaction process both under normal steady-state conditions and off-normal reactor events. As the result of fuel-cladding interaction, iron diffuses into the fuel and forms low-melting eutectic phases. These regions are

at risk of melting during transients if enough iron is present. Lanthanide migration results in cladding weakening, which effectively thins the cladding once the temperature rises beyond the liquidus temperature through eutectic liquefaction [59]. On the other hand, under steady-state operation conditions, Ln fission products tend to migrate down the thermal gradient to the fuel-cladding interface and interact with the cladding, playing a major role in thinning the cladding wall and accelerating cladding rupture, particularly at higher BU [33]. Therefore, a fully mechanistic understanding of FCCI is critical for advanced fast reactor designs.

The formation of low-melting eutectic phases is mainly due to the diffusion of cladding constituent (e.g., Fe) into the fuel rather than the diffusion of fuel components (e.g., U) into the cladding. Fe diffusion into the fuel reduces the fuel solidus temperature [60]. The primary effect of low-melting eutectic phases formation on the fuel element is to cause liquefaction penetration into cladding during transient overheating events [25, 57]. Of particular concern is the formation of a U-Fe phase, which has lower melting temperatures than the fresh fuel, thereby reducing the margin of fuel melting at steady state or accelerating cladding failure under elevated temperatures [61]. UFe_2 and U_6Fe are the key components in the eutectic penetration causing HT9 cladding failure in a metallic fuel relocation experiment [62]. Phases of fission products are also of interest as fission products accumulate at the fuel-cladding interface. Besides contributing to cladding thinning, Ln fission products (typically Ce and La) can form low-melting phases with Fe (or Ni) from the cladding [63], particularly at high BU. The eutectic melting temperature of Fe-Ln compounds could be very low (for example, FeCe is 592◦C and Ni/Ce is 483◦C) [64]. Eutectic phase formation is highly temperature dependent. Depending on the fuel and cladding materials, the onset temperature of forming fuel-cladding eutectic phases varies from ∼700 to 725◦C. The eutectic formation temperature between a selected fuel and cladding puts operational limitations onto the coolant outlet temperature [65]. Matthews et al. [66] distilled the relevant melting experimental results as a function of plutonium in Figure 3-7.

FCCI and eutectic penetration are complex phenomena that depend on the local fuel and cladding compositions, linear power rating, BU, and cladding temperature that vary at different stages during the fuel element lifetime [63]. Adding Zr into the fuel tends to increase the eutectic threshold temperature while the appearance of Pu and lanthanide fission products tend to decrease the eutectic threshold temperature. For instance, previous U-Pu-Zr-Fe diffusion couple studies confirmed that the liquefaction threshold temperature was between 942 and 963K in the U-16Pu-10Zr-Fe couple and between 963 and 983K in the U-9Pu-10Zr/Fe couple [73]. Kim et al. [74] reported the study of microstructure and eutectic penetration rate on an irradiated metallic fuel (U-10Zr) slug with T92 cladding after a high-temperature heating test (maximum temperature of 1200◦C). The measured penetration rate for the irradiated metal fuel is higher than that for the unirradiated U-10Zr specimen. This is because lanthanide fission products tend to migrate down the thermal gradient to the fuel-cladding interface and lower the eutectic penetration threshold temperature.

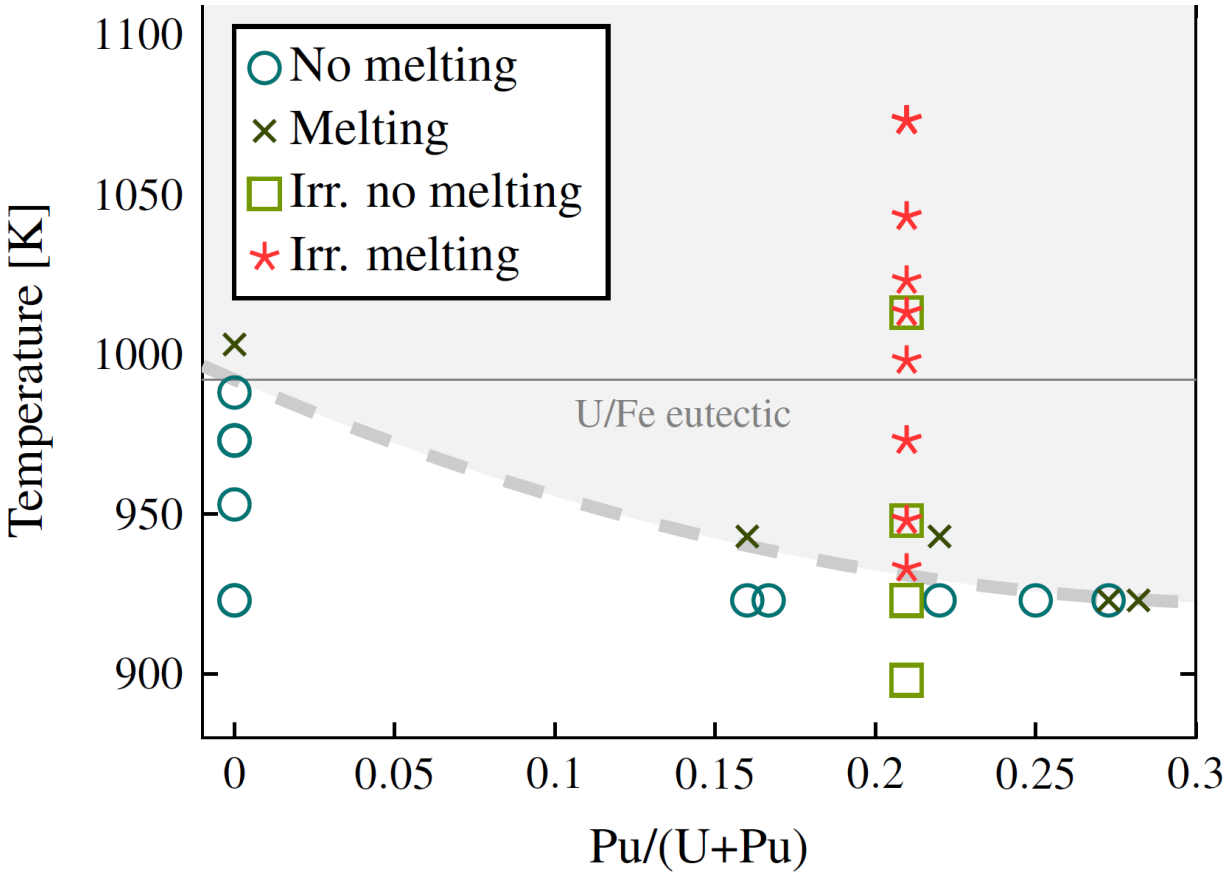

Figure 3-7 Empirical Relationship between the Relative Atom Fraction of Plutonium and Fuel Melting, where the Circles and x's Are from Diffusion Couple Studies [67, 68, 69, 70, 71, 72], and the Boxes and Stars Are from Annealing Experiments using Irradiated Fuel [63]

A wide range of in-reactor transient tests [75] and out-of-reactor furnace heating experiments explored the transient performance of metallic fuels in the IFR program. A series of tests, named M-series, has been performed at the TREAT facility to probe the cladding failure threshold during transient overpower events [75]. These experiments found that cladding failure in BUs under 2 at% was caused by eutectic penetration, in 2–7 at% by the combination of partial eutectic penetration and pin plenum overpressure, and above 7 at% by pin plenum overpressure.

A literature review summarized some early experiment efforts to explore the BU and operating parameters effects on the fuel surface liquefaction threshold temperature for U-Pu-Zr/HT9 systems [60, 63]. Basically, the liquefaction threshold temperature lowers as BU increases. An early study found that the region of eutectic melting coincides with the depth of the Fe penetration into the fuel. Initially, eutectic melting results from the Fe already in the fuel due to interdiffusion upon irradiation. Extensive eutectic melting requires more Fe diffusion from the cladding during off-normal events. It took minutes to have enough Fe in the fuel at elevated temperatures to cause liquefaction in fuel. The fraction of fuel where the liquid phase exists is typically small and primarily restricted in the periphery unless the temperature is very high (above 800◦C) or time duration goes up to hours long. The cladding penetration rate obeys the

Arrhenius temperature dependence from the liquefaction threshold to 1080◦C. Above 1080◦C the rate will be accelerated by several orders of magnitude so that the cladding failure is almost instantaneous.

There are two major research strategies to experimentally investigate FCCI phenomena: in-reactor irradiated fuel pin sample PIE through a variety of characterization techniques and an out-of-reactor diffusion couple study of fresh fuels to investigate thermal diffusion characteristics with no contribution from radiation. PIE studies provide first-hand experimental data for understanding the FCCI microstructure and composition of neutron-irradiated fuels. A large amount of PIE data, including the FCCI zone width and compositional characterization, has been collected from EBR-II irradiated fuel elements (U-Zr and U-Pu-Zr with HT9, D9, SS316 cladding). The maximum FCCI zone thickness ranges from 70 to 170 μm for HT9-clad U-10Zr irradiated at a BOL fuel-cladding temperature of 660◦C up to 5.0–10.0 at% BU. For HT9-clad U-Pu-10Zr irradiated at around a BOL fuel-cladding temperature of 550◦C to about 10 at% BU, the max FCCI thickness was about 40 μm. More information can be found in the literature [76]. A previous study of EBR-II irradiated fuel pins discovered that Ln fission products, particularly neodymium (Nd) and cerium (Ce), have been identified in high concentrations at the fuel-cladding interface and make major contributions to FCCI [77]. The Ln fission products penetrated deepest into the HT9 and D9 cladding. The primary fuel component that penetrated deepest into cladding is Pu for U-Pu-Zr ternary fuel and U for binary U-Zr fuel. Of the cladding constituents, Fe and Ni diffused into the fuel, forming new phases with fuel components. FCCI is highly dependent on temperature and power along the fuel element. The maximum fuel-cladding interaction occurred at the combined high power and high BU region in the fuel pins. Besides, BU is another important factor affecting the FCCI thickness. Higher BU tends to lead to a larger interaction zone. Several reviews focused on improving the understanding of FCCI in U-Zr-based metal fuel systems are available [78, 66, 79].

3.5 Fission Product Behavior and Source Term

Source term is defined, for purposes in this report, as the release of radionuclides to the environment following a severe reactor accident [80]. This is driven by the radioisotope quantity and form in the fuel and by the path leading to the environmental release. Thus, various stages and interactions determine the extent of the release as described in Figure 3-8 by [81] for a SFR. Source term analyses are of main importance for licensing requirement under various accident events and relate to an entire reactor, thus may not be fully bound herein. As the entire reactor is involved in the response actions taken after a fuel breech (such as the extension of the evacuation and exclusion zones and decontamination actions), it should be noted that only the fuel system can be assessed here and further source term determination must be made outside of the scope of this work. While substantial work exists for light-water reactors and guidelines for source term determination are provide in [82], limited work exists for SFR.

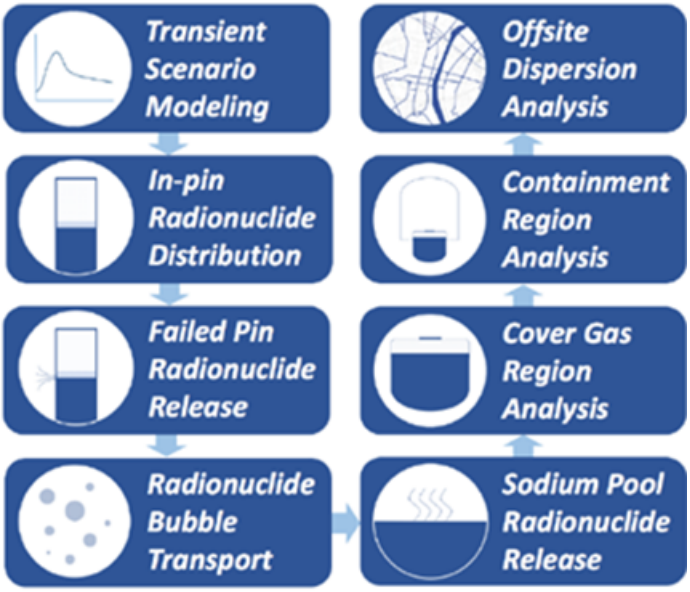

Figure 3-8 Example of Stages and Information Needed for the Calculation of Source Term in a SFR, as Reported in [81]

Different barriers exist to radioactive release to the environment in a SFR (fuel, clad, sodium, primary circuit, containment) [83], when performing source term analyses the behavior of the radionuclide of interest must be analyzed in all transport phases (from fuel to containment and following to the environment). For a correct source term determination, the fission product inventory, chemical form and location at the time of breach must be determined to establish release rates from failed fuel pins and following its release path through sodium to the containment and to the environment, as described in Figure 3-9 by [84].

From the point view of fuel assessment source term is related to radionuclide inventory and chemical form in the fuel at the time of the accident and by the fuel microstructure/chemistry that can influence the path of release. Moreover, source term is strongly influenced by the temperature experienced during the accident and by pin failure mechanism, thus by the accident scenario. Current source term predictions for SFRs are based mostly on knowledge of fission product behavior obtained from PIE analyses based on normal pin operation or from waste refinement experiments, as summarized in a comprehensive literature review [83]. No in-pile tests have been performed for SFR with the sole purpose of studying the source term [80]. Past in-pile tests were conducted at INL-TREAT for metal, oxide, and carbide fuels, and at Sandia National Laboratory's Annular Core Research Reactor 10 (ACRR) for oxide fuels [80]. These were focused mainly on failure mechanism and debris bed coolability, rather than radionuclide release. In fact, towards the end of the first generation of TREAT testing (early 1990's), the IFR program began to realize the potential to answer more of such questions from the M-series tests on metal fuels in TREAT.

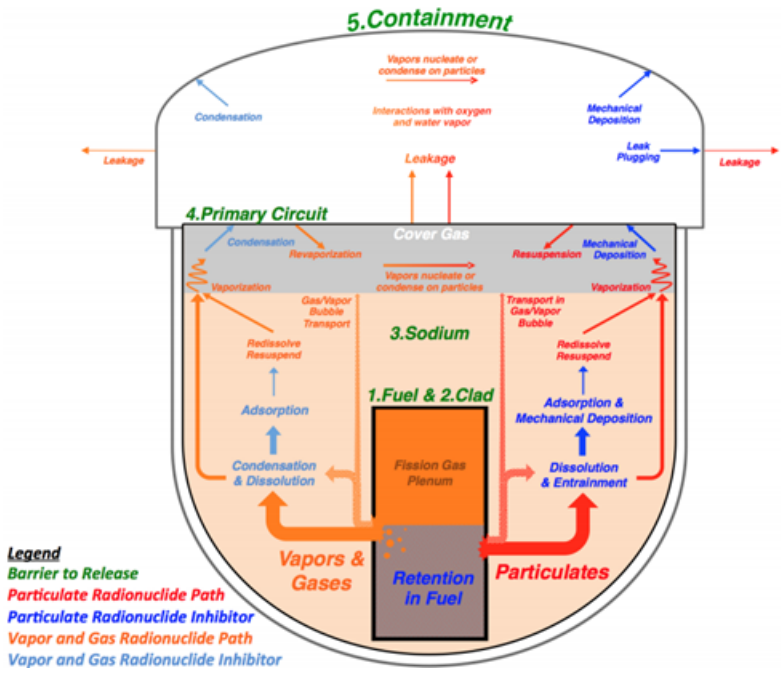

Figure 3-9 Schematic of the Process Involved in the Release of Radionuclides from Fuel Pin to Environment in [84]

During the M-series [84] tests, a prototype online fission product monitoring system was tested in TREAT. The device was based on gamma spectrometry in the void space above the core reflector, monitoring the plenum region of the loops. The results were not satisfactory due to high gamma interference encountered during the transient [85]. Moreover, there have been three past U.S. sodium reactor incidents involving metal fuel that shed light on the possible radionuclide release. From the previously described experiments, an extensive review of fission product behavior for metal fuel fast reactors can be found in the literature [80, 81, 83, 84, 86, 87]. Although these references cover a wide range of metal fuel alloys and compositions the general results can be applied to U-10Zr composition. Indeed fission products can be divided in different classes/groups for source term analyses based on their chemical form and transport behavior as presented in Figure 3-10. The radionuclides of interest for source term include transmutation products, fission products, and actinides due to their extensive radiological consequence.

Characteristics, status and main location of radiocontaminants.

Element	Characteristics in sodium	State in containment	Main location(s)
Noble gases Xe, Kr	Inert, virtually insoluble	Element	Gas phase
Halogens I, Br	React with Na, moderate volatility	NaI, I_2	Na (liq.) Aerosol Gas phase
Alkali metals Cs, Rb	Soluble, high volatility	Cs_2O, CsOH	Aerosol
Alkali-earth metals Sr, Ba	Very low volatility	SrO(s), BaO(s) in liquid suspension	Na (liq.)
Noble metals Ru, Pd, Rh, Ag	Very low solubility (except Ag), very low volatility	Metallic, in suspension	Na (liq.)
Other metals Mo, Tc	Very low volatility	MeO(s), MeO_2(s), Na_2MeO_4(s) in liquid suspension	Na (liq.)
Actinides, U, Pu	Refractory	MeO_2(s) in liquid suspension	Na (liq.)
Others Te	Reacts with Na, moderate volatility, decomposes in contact with air	Na_2Te Te	Na (liq.) Aerosol

Figure 3-10 Fission Product Behavior and Interaction with Sodium as Summarized in [86]

A description of the current knowledge for each class of fission product is provided in the following:

- Noble gases (Xe, Kr) will be released to the plenum at already low burn up (over 2% at.) when pore interconnection occurs. Following a breach of the cladding noble gases can migrate in the sodium and due to their high vapor pressure and low solubility [83], reaching the cover gases. In the cover gas due to the high vapor pressure they will stay in gaseous form and could thus escape to the containment and following to the environment [83]. It is estimated that up to 100% of the inventory of noble gas can be released from a fuel pin. Thus these elements are of major importance to source term determination.
- Halogens (I, Br): the importance of I to source term determination is well known due to its high radiotoxicity, related to its long lived radioisotope (^{133}I) and its retention in the thyroid following a release to the environment and adsorption by humans [83]. However, the chemical form of I in metallic fuel is still under debate [81, 84]. The destiny of iodine following breach of the cladding is tightly related to its chemical form (e.g., UI3 or CsI), which may lead to different behavior during an accident [83]. Up to 100% of inventory can be released from the fuel at very high temperatures (exceeding 1000 ^{o}C). In [83, 86] it is reported that most iodine will probably be absorbed into the sodium liquid becoming sodium iodide (NaI) and will not contribute strongly to the source term. Further studies are thus needed to determine its chemical form and interactions before its release to the environment.
- Alkali Metals (Cs, Rb): Cs affinity with sodium and its presence in the top of the fuel is well demonstrated from current PIE. Its release may reach 10% from the fuel at high (greater than 1000 ^{o}C) temperature. This fission product is believed to remain contained in the primary sodium pool due to its high solubility in sodium, even after breach of the cladding. From the pool to the cover gas its vaporization will be in the order of 10^{-2} – 10^{-4}, with high tendency to re-condense in the colder structural surfaces as reported in [83]. However, in [86] it is suggested that a large fraction of the cesium would remain in the gas phase. Further studies are thus needed to determine its release.
- Tellurium group (Te, Sb): limited data exists for these elements. Refining tests show their high retention in metallic fuel (over 95%), probably due to their low vapor pressure. Moreover, their chemical interaction with sodium and stainless steel may indicate also high retention in the primary system [83].
- Alkaline Earths (Sr, Ba): limited data on the release of these elements exists. Low releases (under 20%) are expected as reported in Ref. [83] due to their low vapor pressure and affinity with oxygen impurity in Na to form oxides in the primary system, even after cladding breach.
- Noble metals (Ru, Mo, Tc, Pd, Rh, Ag, Pt): data are scarce for these elements, but their release is supposed to be limited (under 5%) thanks to their low solubility in Na, high melting point and high adsorption on possible primary surfaces [83].
- Rare Earths (Ce, Y, La): these elements have been observed to react with cladding, forming eutectic. During an accident their low solubility in sodium may imply high retention in the primary system, although its release from fuel may achieve 30%, as demonstrated by previous tests [83].
- Actinides (U, Pu): data on metallic fuel shows compatibility with sodium, even over prolonged time. Release may occur if these elements encountered oxide impurity (e.g., in Na pool) and become soluble in sodium and thus transported to the primary system [83]. However, its release from fuel is expected to be minimal.
- Finally, together with the fission products the release of activated sodium (^{24}Na) must be considered, which could contribute significantly to the radioactive release if the coolant

boundary is lost [80]. In the following Table 3-1 each class of fission products is described based on [83] indicating area which need further investigation.

Table 3-1 Release Expected by Fission Products Classes and the Uncertainties in Their Release As Reported in [83]

		Uncertainties			
Fission Products	Expected Release	Normal Op. ~500°C	Eutectic ~700°C	Fuel Melting ~1100°C	High Temperature ≥1300°C
Noble Gases	High	Low	Medium	Low	Low
Halogen	Debated	Medium	Medium	Medium	Low
Alkali Metals	Low	Low	Medium	Medium	Low
Tellurium Group	Low	Medium	Medium	High	No Data
Alkaline Earths	Low	Medium	Medium	High	Medium/High
Noble Metals	Low	Low	Medium	Medium	Medium
Rare Earths	Low	Medium	High	High	High
Actinides	Low	Low	Medium	Medium	Medium

From the proposed review (derived from [83]) it is concluded that retention is highly possible for most fission products, and that only noble gases could be released to a significant extent (the release from other fission products begin under 10^{-3}). This was also documented in real case scenario in [84]. Some gaps have been however identified for fission products behavior [83, 84] related to their release fraction from failed fuel pins which if resolved could minimize the uncertainties on current source term determination. To respond to these gaps further PIE on available irradiated pins and melt experiments have been suggested [83, 84]. Moreover, the description of transport outside the fuel pin has areas of uncertainties, such as interaction/transport/release and interaction with containment materials.

3.6 Ducting Integrity

There was significant in-reactor monitoring of assembly duct axial growth in the FFTF. The HT-9 alloy has excellent swelling resistance, good creep resistance, and sodium compatibility at temperatures [88]. This work has shown that the HT-9 alloy is nearly free of swelling under high fluence as shown in Figure 3-11 [89], making it the primary candidate for a ducting material. Given that HT-9 swelling is not appreciable at the neutron exposures typical of 10 at% BU (nor is it appreciable at higher exposures), the primary deformation mechanism for HT9 ducts is irradiation creep. Potential loads on assembly ducts might come from fit-up with neighboring assemblies or from position restraints. More important at EBR-II was irradiation creep dilation of ducts due to flow pressure inside the duct; this was not a concern for the thicker-walled FFTF ducts. A loading mechanism such as this should be considered in evaluating the potential performance of ducts in a specific reactor design.

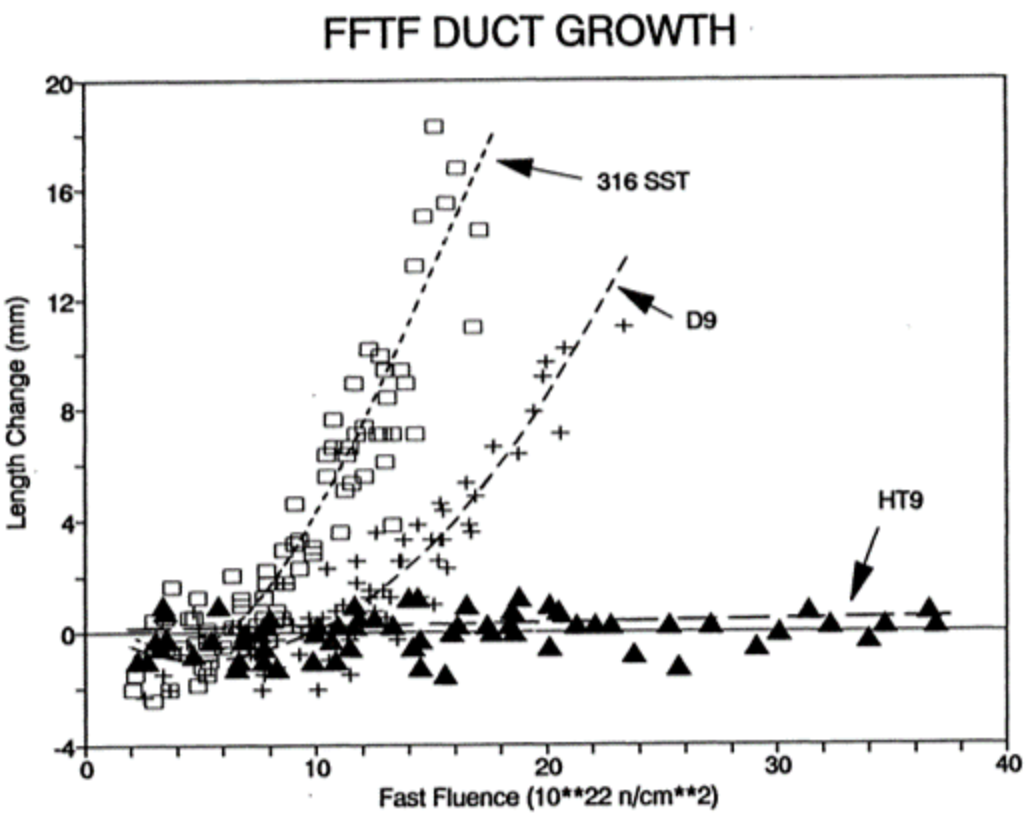

Figure 3-11 Comparison of Assembly (Ducting) Growth in FFTF [89]

3.7 Coolability

As the fuel swells, there is an intrinsic loss of power density, and thus of heat generation. With a 75% smear density and Na bonding, there is no evidence indicating a loss of coolability in the fuel system. As shown in Figure 3-5, the fuel system retains favorable thermal conductivity even with porosity. The geometric changes following cladding contact are predominantly occurring in the axial direction, again lowering effective heat generation, and are limited in the radial direction to under 2% conservatively. While the U-Zr/HT9 system is commonly used with an HT-9 ducting that shows little to no indication of growth, the retention of coolability will be determined by core design. The fuel swelling, represented in prior sections, indicates that the coolant flow can be retained and control rod motion would not impeded by the fuel with proper core designs.

3.8 Transients

Three primary approaches with complementary capabilities (see Figure 3-12) have been used to demonstrate and study the transient performance of metallic fuels:

- The EBR-II facility using a combination of high-temperature subassembly and whole-plant transient experiments [90].
- The TREAT facility using a flowing sodium loop and static capsules to identify phenomenological behaviors and quantify thresholds [75].

- Hot cell furnaces using overheating experiments on pressurized cladding segments to investigate transient stress rupture, fuel segments to measure fuel-cladding eutectic behavior, and whole EBR-II pins for integral thermal effects. These experiments included the Fuel Cladding Transient Tester [55], the FBTA [91], and the Whole Pin Furnace (WPF) [92].

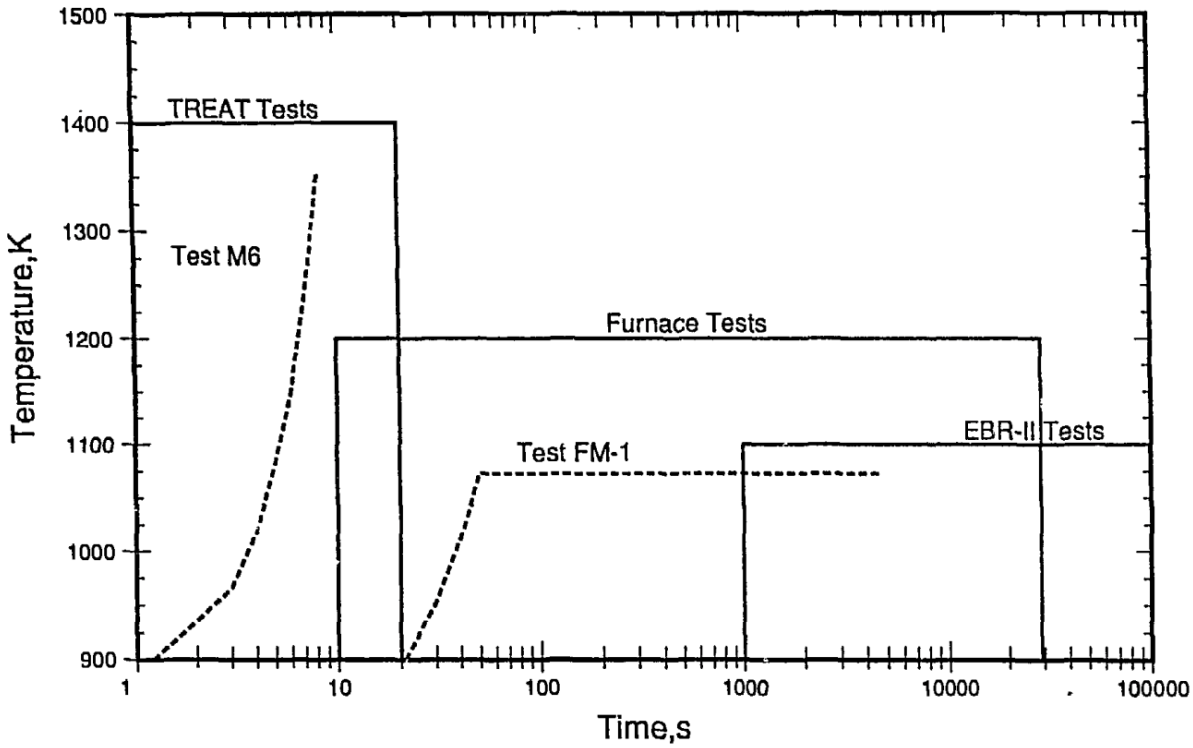

Figure 3-12 Peak Cladding Temperature Regimes for Different Transient Testing Approaches [93]

Early testing started in the TREAT facility on EBR-II Mark-I and IA driver fuels composed of U-Fs but also on Fermi-A U-10Mo fuel [94]. These early phenomenological studies exploring fuel failure thresholds found FCMI and fuel-cladding eutectic penetration dominated fuel damage and failure modes on fresh to low BU pins. FCMI in these early designs was exacerbated by the high smeared density (85% for Mark-I and IA), but the phenomenon has not been consequential in transient testing on later generation designs with lower smeared densities.

In the 1980s, preparation for the Shutdown Heat Removal Tests in EBR-II required qualification testing of the Mark-II fuel design driver core [95]. Out-of-reactor and in-reactor testing was performed to quantify fuel eutectic temperature thresholds and characterize cladding stress rupture. Notably, cladding failure in the irradiated Mark-II design was dominated by a stress riser caused by a dimple placed in the cladding but was removed in later designs. The Shutdown Heat Removal Tests program was composed of 58 individual tests, including an unprotected loss-of-flow event where cladding temperatures exceed the fuel-cladding eutectic threshold of about 715◦C (for the uranium-rich eutectic of concern here). Minor cladding damage was

accumulated, though no fuel failures were detected, and the reactor was restarted immediately after the tests were finished. In addition to whole-plant transient experiments, EBR-II also performed run beyond cladding breach experiments where fuel with defected cladding was irradiated. The experiments included a pin at 12 at% BU operating for 169 days with a breach and another for 223 days, including multiple startups and shutdowns. The experiment results demonstrated no measurable fuel loss or exacerbation of the failure location [90]. This result is due to the good compatibility of the metallic fuel alloy with sodium, which avoids an exacerbation of the failure site in oxide fuel upon a fuel reaction with sodium or water coolant. At the end of the EBR-II program, a series of operational transient experiments was initiated, though only one was completed. This experiment included fuel over 11 at% BU and performed an overpower ramp at 0.1% P0/s to approximately 30% overpower. The experiment showed no negative performance, and recent examinations have shown the fuel shows no detectable change from the pre-transient state [57].

The M-series experiments were performed in the TREAT facility to study fuel failure thresholds under prototypic conditions on single test pins. These tests include six experiments on a total of 15 pins of various compositions. Table 3-2 provides a summary of fuel, experiment, and result characteristics. In this table, normalized overpower is relative to nominal conditions in a fast reactor having a peak linear power of 40 kW/m, 630 K coolant inlet temperature, and 150 K coolant temperature rise. These experiments had single pins in separate flow tubes (isolated thermomechanically). This approach was strategically beneficial for comparing pin to pin results with a direct comparison of differential heat removal performance via flow rate differences between flow tubes. This experimental approach typically provided a unique view of fuel degradation to the brink of and just after failure by triggering the reactor shutdown upon detecting a cladding breach in the hottest pin. The experiment would then cool quickly, “freezing” the fuel state for detailed examination. Due to the relatively high-temperature ramp rates, fuel degradation was found in the fuel-cladding eutectic interaction with some effect of fuel internal pressure to drive some cladding radial distension. Ultimately, any failures were attributed to reaching the iron-rich Fe-U eutectic limit of 1080◦C, a concern for the cladding FCCI. In addition, these tests provided a unique experimental quantification of resulting core reactivity effects via the TREAT neutron hodoscope, which is designed to track fuel motion with millisecond temporal resolution.

Near the end of the IFR program, the WPF experiments were performed at the Alpha-Gamma Hot Cell Facility at Argonne National Laboratory. These furnace tests were developed to simulate longer duration transients more representative of loss-of-flow conditions [25, 60]. Table 3-3 provides a summary of associated test parameters for the seven tests performed on whole irradiated EBR-II pins. These experiments provide additional data over longer times at comparable temperature conditions to the TREAT experiments but show integral effects of fuel-cladding eutectic and cladding overpressure at high temperatures.

Table 3-2 Summary of the M-Series Transient Experiments in TREAT

Experiment	Fuel/Cladding	Fuel Design (EBR-II)	BU, at%	Test Overpower, *Indicates Cladding Failure	Calculated Breech Threshold Overpower (Normalized)	Maximum Fuel Axial Expansion, %	Maximum Pin Pressure, MPa
M2	U-5Fs/316SS	Mark-II	0.3	4.1	4.7	16	0.6–0.8
M2	U-5Fs/316SS	Mark-II	4.4	4.2*	4.5	—	7–9
M2	U-5Fs/316SS	Mark-II	7.9	4.1*	3.6–4.0	3	17–20
M3	U-5Fs/316SS	Mark-II	0.3	4.1	4.8	18	0.6–0.8
M3	U-5Fs/316SS	Mark-II	4.4	4.0	4.4	4	7–9
M3	U-5Fs/316SS	Mark-II	7.9	3.4	3.6–4.0	4	17–23
M4	U-5Fs/316SS	Mark-II	0.0	3.8	4.3	4	7–9
M4	U-5Fs/316SS	Mark-II	2.4	4.1*	4.4	7	2–6
M4	U-5Fs/316SS	Mark-II	4.4	3.8	4.3	4	7–9
M5	U-19Pu-10Zr/D9	X419, X420, X421	0.8	4.3(3.4)	5.1(4.6)	1(1)	1(1)
M5	U-19Pu-10Zr/D9	X419, X420, X421	1.9	4.3(3.4)	5.1(4.6)	2(0.5)	3(3)
M6	U-19Pu-10Zr/D9	X419, X420, X421	1.9	4.4	4.6	2–3	3
M6	U-19Pu-10Zr/D9	X419, X420, X421	5.3	4.4*	4.5	3	10
M7	U-19Pu-10Zr/D9	X419, X420, X421	9.8	4.0*	4.4	3	19
M7	U-10Zr/HT9	X425	2.9	4.8	4.4	2–4	6

The database of experiments from the WPF (maintained in the out-of-pile transient database [96]) and the TREAT M-series provide a good experimental validation basis for fuel behavior to failure. The tables show that only one U-10Zr fuel composition in HT-9 cladding was tested in each facility. However, the results indicate performance phenomena are consistent with the other tested fuel types and the separate effects testing for specific compositions in the fuel-cladding eutectic in the FBTA and cladding stress rupture. It is notable that the single U-10Zr pin tested in the TREAT facility was predicted to fail but did not. This result was attributed to the higher liquidus temperature of the alloy. The FBTA was the primary experimental approach providing a detailed study of the fuel-cladding eutectic interaction. The setup heated short, irradiated fuel segments of various compositions, cladding types, and fuel operating characteristics to target temperatures held for specific periods of time. Cohen et al. provide an overview of key conclusions of results from the FBTA [97] while Denman provided a detailed

state-of-the-art results summary and analysis [98]. While operating history such as BU, cladding temperature, and linear power may play a role in defining a specific threshold, the penetration rate does not seem to be impacted much. Data as presented in Reference [97] shows fuel in HT9 cladding BU up to 11%, indicating the temperature threshold for eutectic formation. The Fuel Cladding Transient Tester was used to measure transient stress rupture in defueled, pressurized segments of stainless steel and HT9 claddings [99]. Kramer et al. summarized the data and evaluated derived models against WPF tests [25]. A variety of fuel compositions and claddings were tested through a variety of approaches, providing a complete understanding of fuel degradation phenomena. However, some fuel designs were tested in limited quantities in integral experiments. The combination of similar properties and behavioral phenomena of alloy variants and separate effects testing provides a justification of performance within the envelopes tested. The maximum BU tested in furnace testing is approximately 13 at%, also justifying a BU limit of near 10 at%.

Table 3-3 Summary of the FM-Series Out-of-PileTransient Experiments in the Alpha-Gamma Hot Cell Facility

Experiment	Fuel/Cladding	Fuel Design (EBR-II)	BU, at%	Test Temp. (°C)	Duration (min)	Eutectic Penetration (% cladding thickness)	Peak Strain (%)
FM-1	U-10Zr/HT9	X425	3	820	97, failed	64	3.3
FM-2	U-5Fs/316SS	X425	3	820	112, failed	67	2.3–4.3
FM-3	U-5Fs/316SS	X425	2.2	820	146, failed	65	1.2
FM-4	U-5Fs/316SS	X430A	11.4	770	68, failed	24	10–15
FM-5	U-5Fs/316SS	X441A	11.4	Ramp to 780, cool	3	0	<0.1
FM-6	U-5Fs/316SS	X441A	11.3	650–670	2,160	0, FCCI	0.89
FM-7	U-5Fs/316SS	X429B	13.5	650–670	2,160	0, FCCI	0.18

4 PERFORMANCE EVALUATION

As shown in Chapter 3, historical data can be used to conclude that U-10Zr in HT9 cladding meets adequate design and safety limits below 10 at% BU and at limited fuel-cladding interface temperatures. In order to show that the fuel meets these criteria before actual operation, fuel performance simulations will inform design and regulatory decisions. In addition, in order to go beyond the operational, design, and manufacturing envelope defined in Chapter 2, fuel performance models—in conjunction with appropriate surveillance and testing—will be a powerful tool to ensure safe operation. To that end, a brief discussion on the state of fuel performance modeling and theoretical understanding is presented here, along with a look into the future of advanced fuel performance modeling. More detail can be found in Reference [10].

4.1 Target Behavior for Modeling Purposes

The fission gas bubble behavior impacts many intertwined parameters essential to fuel performance, and the swelling behavior in the first 1–2% fissions per initial metal atom sets the general microstructure for the remainder of the irradiation [21]. The relatively large porosity leads to thermal conductivity degradation. However, as the porosity becomes interconnected, the bond sodium infiltrates into the fuel, resulting in a partial recovery of the thermal conductivity [100]. Mechanical properties, such as stiffness, fracture strength, and creep behavior, are intimately tied to the porosity distribution as well [101]. As the fuel comes in contact with the cladding, FCMI occurs, creating a complex stress-strain response in the fuel and cladding. Continual swelling due to solid fission products further enhances FCMI, resulting in collapse of the porosity structure due to hot pressing [102]. Furthermore, lanthanides that contribute to FCCI travel down the temperature gradient towards the fuel edge [103, 104]. Recent studies have attributed interconnected porosity as a likely pathway for the lanthanides, tying their ability to collect at the fuel-cladding boundary to the fraction of porosity interconnection [105, 106]. Along with lanthanide transport, cracking in metallic fuels is a primary contributor to FCCI [107]. In order to capture crack locations and extents, an accurate stress profile in the fuel is an essential starting point, of which the bubble sizes and distributions are not only the primary contributor but are intimately coupled to the internal stress.

During irradiation, zirconium migrates radially, resulting in phase boundaries that change as local constituent concentrations evolve. After irradiation, constituent redistribution results in a high Zr γ-phase in the center of the fuel (Figure 4-1c), a low Zr β-phase (or ζ-phase in ternary fuel) in the inner ring (Figure 4-1b), and an α+δ region (or perhaps even a ζ+δ in ternary fuel) on the outer periphery (Figure 4-1a). Despite U-xPu-yZr fuel being used for decades, interpretations of the phase diagram of the binary and ternary fuel forms remain under development and reanalysis (see [108] for more detail). Nonetheless, PIE clearly shows a three-ringed structure in the fuel, which will be referred to here as a high Zr γ-phase, a low Zr β- or ζ-phase, and a low-temperature α+δ phase.

The accommodation of fission gas bubbles in each phase of the fuel is distinctly different; at low temperatures, the orthorhombic crystal structure of α-U results in anisotropic thermal expansion and dose-dependent anisotropic void swelling (Figure 4-1a). This anisotropic behavior depends upon the fuel texturing and can be influenced by fabrication, meaning that novel fabrication methods may experience different swelling behaviors. In a polycrystalline material, such as U-Zr and U-Pu-Zr, this results in cavitation or tears at the grain boundaries [22]. These voids lead to swelling while simultaneously increasing the fuel plasticity. Eventually, fission gas products diffuse to these tears, transitioning the voids to bubbles and stabilizing the pores,

preventing a total collapse of the porosity in these regions due to external stresses.

In the hot interior of the fuel pin, the cubic γ-U phase does not suffer the same anisotropic swelling, but rather is pocketed with fission gas bubbles that develop early under irradiation (Figure 4-1c). The elevated central fuel temperature results in a faster diffusion of fission gas, allowing the bubbles to quickly grow and interconnect. Micrographs at the fuel center indicate large, interconnected bubbles with no grain boundary tearing, which is indicative of rapid fission gas mobility combined with high plasticity to accommodate the fission gas bubble pressure [22]. As the interior isotropically swells due to the growing bubbles, it will promote tensile stresses in the cooler fuel periphery, resulting in fuel creep and preferential swelling in the radial direction. This macroscopic anisotropic swelling was studied extensively in PIE and is observed for all U-Zr and U-Pu-Zr fuels [22].

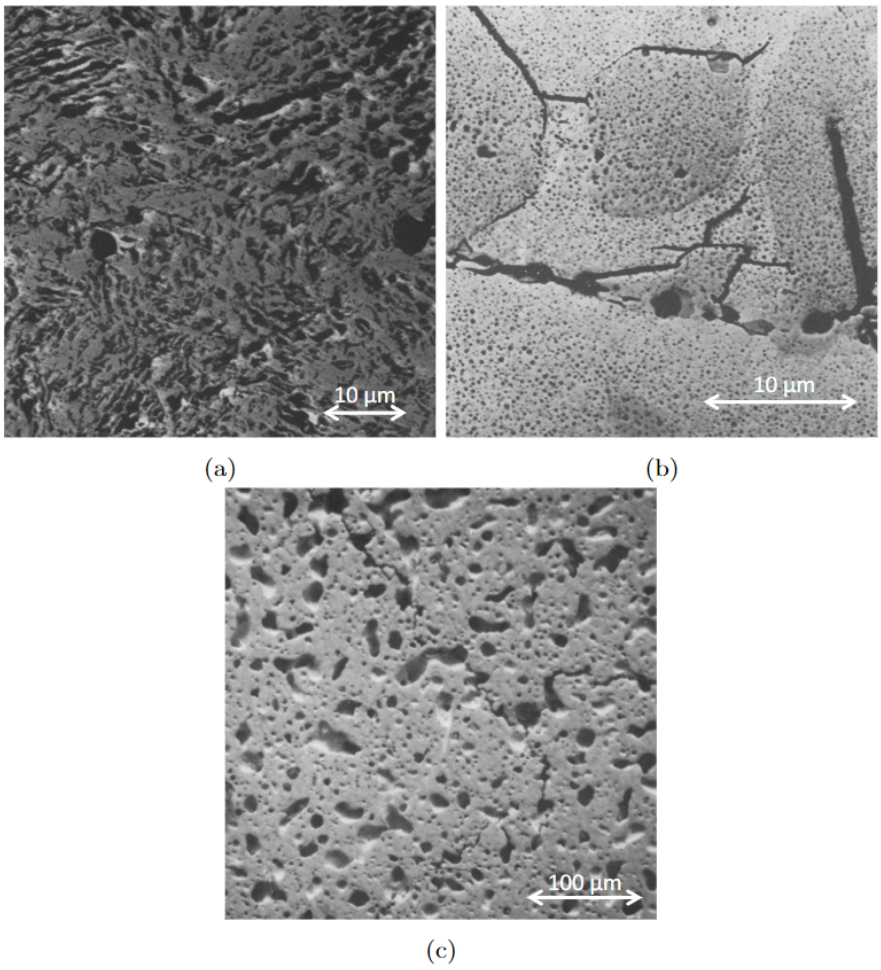

Figure 4-1 Micrograph of the Porosity Observed in a) ζ+δ, b) ζ, and c) γ Phases in Irradiated U-xPu-yZr fuel [22]. Note that Scales Are Not Preserved between the Pictures.

Between the high Zr regions in the fuel center and rim, the β-phase (or ζ-phase in ternary fuel) retains a much denser appearance from many small bubbles with small fractures running across

the region (Figure 4-1b). This high-uranium density fuel region likely experiences extreme stress profiles due to the surrounding phases; that is, the β-phase region is squeezed between the γ-phase swelling and cold α+δ-phase [22].

4.2 Fuel Performance Modeling

4.2.1 Introduction

Metallic fuel simulations have provided information to both core and experimental designers for decades [109]. Early models were developed by leveraging data to produce descriptive empirical correlations [110]. These initial simulations provided a code for the confirmatory analysis of experimental assemblies in EBR-II, a scoping tool for reactor designers for the EBR-II successor, the IFR, and are even used now to help provide simple safety calculations for yet-to-be-built fast reactors [111]. While these “descriptive” models are useful within the experimental data envelope from which they were derived, they often are not appropriate when applied to designs or operating conditions outside the bounds described by the data. In order to provide a tool that can predict the behavior of metallic nuclear fuel beyond familiar conditions and designs, a set of mechanistic models need to be developed to develop confidence in simulation results outside of known experimental data points [112].

As a consequence of increasing computing power combined with improved computational methods underpinned by modern fundamental material science understanding, the ability to model fuel rods “from atoms to pins” may soon reach fruition [113]. Starting at the smallest of time and length scales, density functional theory can quantify defect energies and diffusion [114, 115] and fundamental material characteristics [116, 117] and helped predict the performance of nuclear fuel beyond the envelope of irradiation data [118]. Using density functional theory derived data, empirical potentials employed in molecular dynamics simulations have led to a fundamental understanding of irradiation damage [119, 120, 121], athermal diffusion [122, 123], and bubble-in-solids behavior [124]. On the microstructural scale, the material response due to irradiation at high temperatures have been explored with crystal-plasticity models, which have been used for complex grain behavior simulations [125]; cluster dynamics simulations, which have been used to track the defect concentrations and their interaction with other defects [126, 127, 128, 129]; and phase-field simulations to track the percolation of fission gas in solids and other thermo-dynamic behavior [130, 116, 131]. Lastly, developing advanced models in thermo-mechanics and thermo-dynamics [132, 133, 134, 135, 136], along with informing these more complex models using lower-length derived information, has seen success in informing engineering-scale simulations using the Multiphysics Object-Oriented Simulation Environment (MOOSE) [137] and its derivative fuel performance code BISON [138, 139].

For the baseline metallic fuel design outlined in Chapter 2, engineering-scale models (e.g., BISON) can typically capture fuel behavior. Bolstered by MOOSE’s flexibility [137], the development and application of mechanistic thermomechanical simulations within the BISON fuel performance code [138, 139] have accelerated in recent years. BISON is a modern finite-element-based, multidimensional fuel performance code developed by the Nuclear Energy Advanced Modeling and Simulation Program under the U.S. Department of Energy, Office of Nuclear Energy. The code capabilities have been developed, utilized, and verified by multiple organizations.

Many tools have been developed to model zirconium-based metallic fuel, with varying levels of success, validation, flexibility, and availability. Here, the capabilities in BISON [138] and those inherited from the MOOSE [137] will be used to frame the following discussion on fuel

performance modeling of metallic fuel. What follows is a brief overview of the equations solved for general U-xPu-yZr fuel performance simulations and some of the specific material properties and models implemented in BISON. In general, these principles are shared across all fuel performance codes.

4.2.2 Problem Definition

Fuel performance simulations essentially focus on the thermomechanical-chemical performance of the nuclear fuel pin, here defined by everything within the cladding envelope, including the fuel, cladding, fill gas, and bond sodium (Figure 4-2). Simulations solve for temperature, *T*, displacements, *u*, and chemical species concentration, *X*. Energy deposition from fission is estimated either through reactor power measurements, or calculated externally using neutronics codes, and is provided as a heat source term, $\dot{q}$. A heat flux boundary condition captures the heat removal from the outer cladding surface by the coolant, which increases in temperature as it flows past the cladding. Displacement boundary conditions axially fix the bottom of the cladding, and the fuel mesh is stitched (i.e., maintained as a continuous, non-breaking finite-element mesh) to the stand mesh, allowing the fuel to grow and impart a force on the cladding via mechanical contact algorithms on the cladding inner surface. In addition, pressure boundary conditions on the interior and exterior of the cladding are applied, representing the plenum and coolant pressure respectively. Finally, thermal flux boundary conditions are utilized to provide thermal "contact" between the fuel outer surface and cladding inner surface.

In a real fuel pin, liquid sodium fills the gaps between fuel and cladding. Thermal contact algorithms between fuel and cladding only account for radial heat flux, resulting in a sharp temperature discontinuity at the top and bottom fuel surfaces where conduction would act to remove heat from the fuel via the bond sodium. In order to capture a more realistic temperature profile—and better behaved physics to ease computational expense—artificial "cap" and "stand" mesh blocks are stitched to the fuel top and bottom, respectively, with liquid sodium thermal properties, and thermal flux contact linkages with the inner cladding surface. The stand is also stitched to the inside surface of the cladding bottom, while the cap can freely axially expand. Since the bond sodium imparts no tangible mechanical constraint on the fuel or cladding beyond pressure, mechanics are not solved in the cap and stand. In order to propagate displacement information and allow for fuel expansion, artificial diffusion is applied to smooth the x and y displacement variables in the cap and stand.

Following this general problem description, the partial differential equations that are solved are,

$$0 = \rho(T,X)c_p(T,X)\frac{\partial T}{\partial t} - \nabla \cdot \lambda(T,X)\nabla T - \dot{q}(X), \tag{4.1}$$

$$0 = \nabla \cdot \sigma + g, \tag{4.2}$$

$$0 = \frac{\partial X}{\partial t} - \nabla \cdot D(T,X)\nabla X - \nabla \cdot S(T,X)\nabla T. \tag{4.3}$$

Eq. (4.1) describes the typical heat equation with source term, where t is time; ρ, c_p, and λ are the density, heat capacity, and thermal conductivity of the material; and $\dot{q}$ is the heat source term. The material properties are dependent on the temperature and constituent concentrations. Eq. (4.2) describes the stress divergence, where σ is the stress tensor and g is the gravitational body force. Finally, Eq. (4.3) is the species diffusion balance equation, where D and S are the temperature- and constituent-concentration-dependent Fickian and Soret diffusion coefficients, respectively [140, 141, 142].

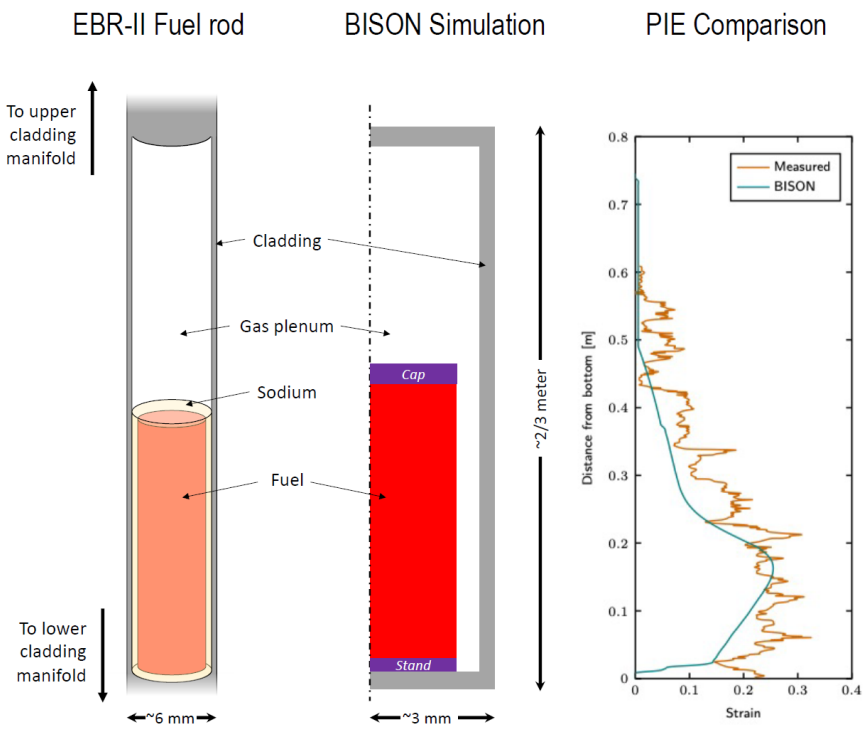

Figure 4-2 Sketch of a Typical EBR-II Metallic Fuel Pin as Built (Left), as Modeled in 2D-RZ (Middle), and Compared to Simulation Data (% Strain) to Measured Axial Profile. Note, This Figure Is Not to Scale. Spacing between the Fuel and Cladding Is 0.35 mm for Most Irradiations of Interest. The Metallic Fuel Pins Irradiated in FFTF Were Three Times as Long but Otherwise Had Similar Geometry. The Cap and Stand in the BISON Simulation Replicate the Smooth Temperature Profile through the Bond Sodium Above and Below the Fuel.

4.2.3 Nuclear Core Environment Models

The neutron flux present in the fuel during irradiation is dependent on local conditions—constituent concentrations, isotopic neutron cross sections, and temperatures—as well as the global condition and response of the reactor. Simulations have previously modeled the flux and fission rate in EBR-II fuel [143]. Unfortunately, the complexity of such calculations makes it difficult to fully incorporate them into fuel performance simulations. In lieu of a coupled 3D neutronics calculation, the local fission rate density can be estimated based on the rod linear power, axial power profile, and power ratio computed for local constituent concentrations. Given the localized fission rate density in the fuel, the local heat deposition can be computed by multiplying the fission rate density by the energy per fission and total fission heat deposited in the fuel.

The constituent models used to describe the response of the cladding often include a dependence on the flux, fluence, or displacements per atom (dpa) that result from damage due to fast neutrons (above 0.1 MeV). The fast neutron flux can be estimated via the fission rate density and macroscopic fission cross section of the fuel estimated from the initial fuel isotopics. The total fast neutron fluence is the time integral of the neutron flux, and the dpa is the fluence (or flux for dpa rate) divided by 2×10^{21} [n/cm^2 per dpa] [144].

The EBR-II reactor had an axial power profile in a typical “chopped cosine” shape, with the peak flux slightly below the core mid-plane. A third-order polynomial can account for this axial profile when calculating the fission rate, fast flux, and coolant channel models.

In EBR-II, the sodium coolant flows past the fuel at a rate set by orifices at the bottom of each fuel assembly. The coolant flow moves freely between fuel pins within the same assembly but is isolated from all other assemblies by a hexagonal duct that encompasses each individual assembly. As the sodium coolant moves from the bottom to the top of the core, it removes energy from the fuel pins and increases in temperature. Thermal-hydraulic simulations have previously modeled the increase in coolant temperature as it moves past the fuel pin [143]. As a first approximation, the heat deposited by a single fuel rod can model the increase in coolant temperature from an assembly flow rate and inlet temperature. Although this adiabatic assumption does not account for mixing between adjacent coolant channels, it provides a simple estimate for the coolant temperature boundary condition required for fuel performance simulations without the need for complex coupled simulations.

4.2.4 Pressure Boundary Conditions

The gas plenum above the fuel and fill sodium in a typical EBR-II fuel design exerts some pressure onto the fuel slug and, more importantly, on the cladding inner surface. If the plenum is too small, fission gas that accumulates during irradiation can result in high cladding stress, leading to large deformations and eventual cladding failure. During assembly, a helium backfill is included in the gas portion of the fuel pin, partially to minimize the stresses imparted by the coolant at the BOL. This backfill pressure is typically 80 kPa.

As the simulation progresses, fission gas released from the fuel pin increases the plenum pressure. The ideal gas law is typically used to calculate the increasing pressure given the estimated fission gas release. In addition, the plenum volume evolves during operation due to differing thermal expansion between the fuel, cladding, and bond sodium, as well as fuel swelling and eventual partial pore infiltration of bond sodium. Finally, the pressure due to the sodium coolant on the outside of the pin is estimated to be 345 kPa, the pressure at the inner-core sodium inlet [145].

4.2.5 U-xPu-yZr Specific Models

The key models needed to capture the fuel performance of metallic nuclear fuel are specific thermomechanical properties and models to capture fission gas bubble behavior. Many models exist for material properties of U-xPu-yZr fuels that try to stitch together the few available data points into a reasonable relationship that reproduces the observed fuel behavior. Unfortunately, many properties lack correlations across the full spectrum of constituent concentrations (i.e., for all x and y in U-xPu-yZr). Due to zirconium migration, a single fuel pin may experience between 5 and 50 at% of zirconium throughout the radius of the fuel slug; thus, correlations that allow for such a large range are required. Ideally, the multiphase state of the fuel during irradiation motivates new correlations based on temperature and phase.

4.2.5.1 U-xPu-yZr Thermal Properties

There are several correlations for the thermal conductivity of U-xPu-yZr fuels [146, 147, 148, 140, 101, 149, 150, 151, 152, 153]. The model utilized by BISON is similar to the models used by References [151, 140], re-evaluated across a wider swath of data in order to capture the full

range of zirconium and plutonium concentrations. The model is built of individual constituents, with mixing corrections calibrated against available data [154, 155, 156, 157, 158, 159, 160, 161, 162, 163, 164, 165, 166]. Although complicated, the BISON model results in a standard deviation of less than 1.3 W/m/K when compared to the data (see Figure 4-3) and is relevant for all compositional space below w_{Pu} = 50% from room temperature to 1200 K.

The onset of porosity interconnection results in sodium infiltration into the fuel. A formulation for the porosity correction to the thermal conductivity due to gas- and sodium-filled porosity has been adopted from Reference [100] and can be coupled to the fission gas bubble interconnectivity model.

A handful of specific heat correlations have been used in past analyses [167, 148, 147, 146]. The model typically used is from Savage, [167], which provides a bilinear fit as a function of temperature for the α + δ low-temperature region, and a high-temperature γ region. A simple linear interpolation is used for the β + γ region (i.e., between $T_{\alpha,\delta}$ and T_{γ}).

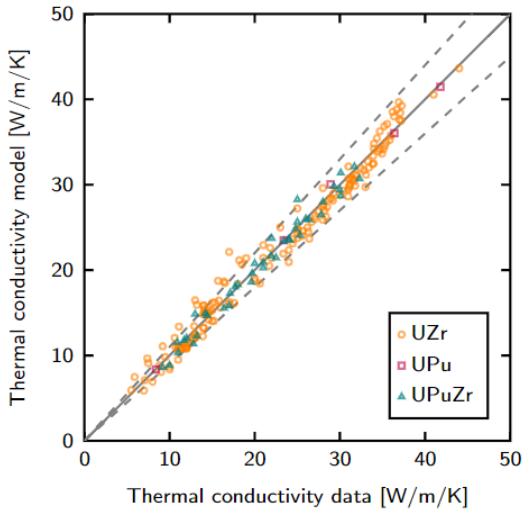

Figure 4-3 Comparison between Model and Data for the Thermal Conductivity of U-xPu-yZr fuel. The Solid Line Represents a Perfect Representation, and the Dashed Lines Represent a ±10% Deviation.

4.2.5.2 U-xPu-yZr Mechanical Properties

The value for the Young's modulus of U-xPu-yZr is typically computed via the correlation by Hofman et al. [168]. In light of new data and understanding of the U-xPu-yZr fabrication process since that model was originally formulated, a new correlation has been developed and implemented in BISON based on a set of U-Zr [169, 170] and U-Pu-Zr [163, 171, 172, 147] data that is applicable across a wide swath of temperatures and constituent concentrations. This new formulation performs more favorably than the model from Hofman et al. [168], especially for the high-temperature plutonium-bearing fuel, as shown in Figure 4-4. Such a fit should be applicable to both cast and extruded slugs as long as the material texture is consistent.

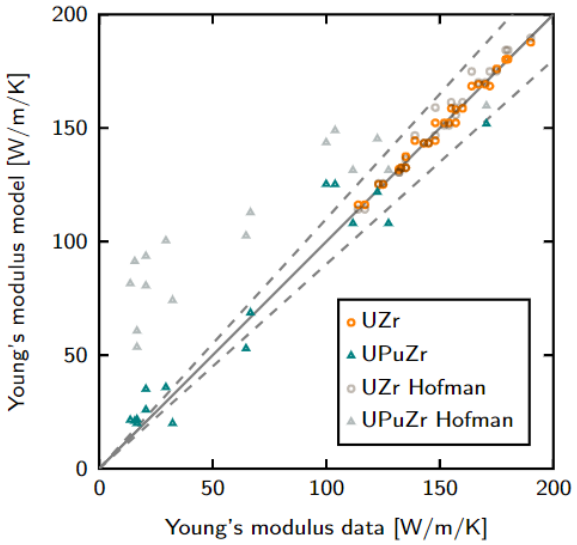

Figure 4-4 Comparison between Model and the Data for the Young's Modulus of U-xPu-yZr Fuel, Including the Correlation from Hofman et al. [168] as Implemented in BISON. The Solid Line Is a Perfect Representation, and the Dashed Lines Represent a ±10% Deviation.

The correlation for Poisson's ratio, ν, for U-xPu-yZr fuel is formulated using temperature- and constituent-concentration-dependent correlations from Hofman et al. [168].

The constitutive model for the thermal and irradiation creep of U-xPu-yZr fuel is taken from Hofman et al. [168], who provide a correlation for thermal creep strain rate for the α + δ and γ phases, and a general irradiation-induced creep strain rate.

4.2.5.3 U-xPu-yZr Strains

The swelling behavior of the metallic fuel is highly complex due to the relatively large pore sizes, the phase dependence of the material properties, and the interconnected behavior of porosity with all other fuel properties. From the most basic description of strain due to fission products, the fissioning of a single uranium or plutonium atom results in two new atoms. If all atoms had equal volumes, this would lead to a strain equal to double the BU (e.g., 2% strain from 1% fissions per initial metal atom). In reality, the noble gases, which account for about 25% of fission products, tend to accumulate, requiring an increasing volume per atom as bubbles get bigger. This naturally leads to a separation of the total swelling of the fuel into solid and gaseous contributions.

Although in principle there are many factors that impact the strain induced by solid fission products, the sensitivity to such factors tends to be minimal [173, 174]. Consequently, the solid swelling rate is typically assumed to be 1.5 times the BU, as suggested by Reference [173], to represent the experimental observations of U-xPu-yZr fuel. In general, the solid fission product swelling is not the dominant swelling mechanism until high BUs are achieved.

Despite the importance of fission gas behavior in metallic nuclear fuel, it tends to be notoriously difficult to capture in a simulation. Many empirical correlations exist for fission gas swelling [175, 176, 102, 177, 178], which perform adequately within their envelope of applicability. In general, the swelling due to fission gas bubbles is related to their number (i.e., concentration distribution) and size; typically, either parameter is fixed in fission gas models based on empirical observations or estimates, while the other is a free variable that depends on the absorption of gas atoms by the bubble. Where these models start to fail is during off-normal conditions, such as annular fuel, axially varying constituents, or operational transients. In addition, the more fundamental fuel properties, such as the interconnection fraction and size distribution of the bubbles, are unavailable with many of the ad hoc models. The approach taken here is an interconnectivity-centric fission gas swelling model that utilizes a series of simplifying assumptions to match expected fuel swelling and fission gas release in a semi-empirical manner. In order to provide a baseline comparison as advanced mechanistic relationships are implemented into BISON, the model utilized here uses several approximations to formulate a simple swelling and fission gas release model. While these simplifications provide adequate comparisons to EBR-II irradiations, there is a clear need for a more mechanistic formulation.

The baseline fission gas model used in BISON was originally introduced by Olander [179] and essentially assumes rapid diffusion, resulting in a fraction of produced fission gas that is immediately born inside bubbles in the fuel, with the remaining fraction being retained in the fuel lattice. The fission gas bubbles, which are defined with initially zero volume and a constant density, grow as a function of local BU and remain perfect sinks for the gas. Assuming that the local bulk stress state does not impact the bubble size, the pressure exerted by the gas is assumed to be in equilibrium with the surface tension of the bubble via the Young-Laplace equation. Here, the model assumes the ideal gas law, which is reasonable for the large bubbles observed in metallic fuel. With this, the volumetric strain due to bubble growth becomes a simple analytical expression.

Although simple, the rapid diffusion model results in an adequate correlation to experimental data by calibrating some of the key parameters. In reality, the bubble sizes will depend on the local stress state of the fuel, fission gas diffusivity, and perhaps even vacancy diffusion, all of which motivate a more complicated model to capture the material response.

In general, the swelling due to fission gas bubble growth will terminate once the bubbles become interconnected with an outside surface and their contents vent to the fuel plenum. Any further gas that reaches the now empty voids is assumed to instantly vent to the plenum. The interconnection fraction is assumed to be related to the porosity smooth function. Again, interconnected porosity is assumed to be in direct communication with the plenum gas, (i.e., percolation of locally interconnected porosity to an outside surface is assumed to be instantaneous). This is due to observations of irradiated metallic fuel that showed many interconnected pathways throughout the fuel via radial and axial cracks and large swaths of interconnected porosity. In addition, bubbles are assumed to retain their shape and size once they become interconnected. In reality, axisymmetric hot pressing of the pores occurs, resulting in a complex distribution of pore shapes and sizes [22].

U-xPu-yZr exhibits anisotropic strains, swelling much more in the radial than in the axial direction [180]. Capturing this effect requires a mechanistic fission gas swelling model that couples to the local stress state of the fuel in conjunction with phase dependence. In lieu of a complex model, a simple anisotropic scaling factor can be used to empirically capture the radial fuel growth.

In addition to fission product swelling, thermal expansion results in a stress-free strain on the fuel. Following a similar procedure as for the thermal conductivity and Young's modulus models discussed in Sections 4.2.5.1 and 4.2.5.2, a new thermal expansion correlation has been developed that encompasses a wide range of constituent concentrations. This correlation has been calibrated against data for U [181], U-Zr [182], and U-Pu-Zr [183, 166] alloys. Using these new correlations, the thermal expansion can be calculated for U-xPu-yZr with a standard deviation of 0.04 when compared to data that spans 0–20 wt% Zr and 0–26 wt% Pu. Figure 4-5 shows the deviation of this new model from the data for U, U-Zr, and U-Pu-Zr.

As the fuel contacts the cladding, FCMI starts to impart compressive stress on the fuel. As irradiation and solid fission product swelling continues to volumetrically grow the fuel, the porous fuel starts to experience hot pressing, or pore collapse. Without treating the pore collapse, the solid fission product swelling of the fuel leads to either extrusion into the upper plenum or extreme strain on the cladding. Like gaseous swelling, this strain contribution is difficult to capture mechanistically, requiring polycrystalline lower-length-scale models to capture accurately, although generalized models exist for the constitutive behavior of porous materials that have been adapted here [184, 185].

Through the study of hot-isostatically pressed U-10 wt% Zr samples, McDeavitt and Solomon [186] developed a densification model to calculate the rate of pore collapse in porous metallic fuel. The hot pressing plastic strain rate they defined is a combined diffusion-controlled cavitation, established by Speight and Beere [187, 188]. This is combined with a creep-flow model established by Needleman and Rice [184], which is further refined by Chen and Argon [189]. Although lacking a fully mechanistic development, especially with regards to phase-dependent microstructures and properties, this hot pressing model can be adapted as a first attempt to capture pore collapse. The model details are reproduced below with small refinements to make it applicable to the BISON simulations.

In order to compute the gas content in the bubbles, a fission gas inventory method must be adopted. Starting with gas production, the total gas content can be computed from the fission rate density. In the simplest model, a fraction of the gas is assumed to always be dissolved in the fuel lattice. As fission gas diffuses into bubbles, which eventually interconnect and release their contents to the plenum, the fission gas release is calculated as the release from interconnecting bubbles and losses due to gas diffusing to interconnected bubbles.

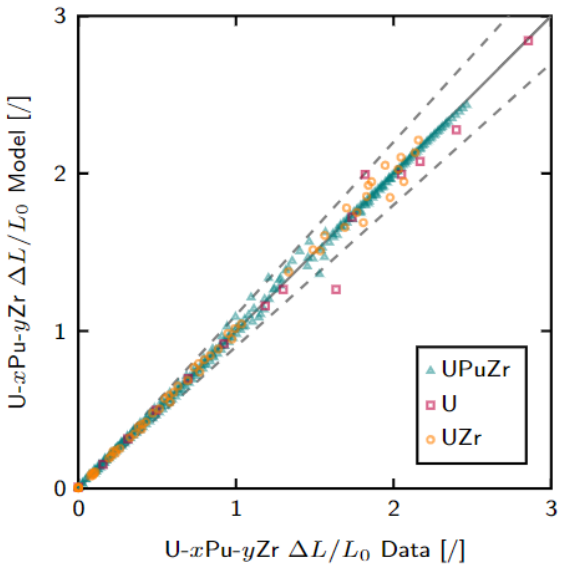

Figure 4-5 Comparison between Model and Data for the Thermal Expansion of U-xPu-yZr Fuel. The Solid Line Represents a Perfect Representation, and the Dashed Lines Represent a ±10% Deviation.

4.2.6 Cladding Specific Models

U-xPu-yZr was typically clad in SS-316, D9, or HT9 steels during irradiation in EBR-II and FFTF. Due to the improved irradiation resistance of D9 and HT9, these two types of cladding materials are primarily used in the experimental assemblies of interest here. The fundamental thermomechanical properties of these materials are the thermal conductivity, specific heat, creep—both thermal and irradiation enhanced, and void swelling. Fortunately, the extremely low swelling behavior of HT9 allows void swelling to be ignored, with the creep behavior as the key component required for fuel performance simulations.

4.3 Discussion

One of the biggest missing pieces in the simulations shown here is the absence of constituent redistribution. Several models have been implemented for zirconium migration, with varying degrees of success [140, 190, 141, 191, 192, 193, 194, 195]. While important, only a subset of the models utilized in the baseline BISON capabilities are dependent on concentration; thus, the added computational cost is not fully justified. Ultimately, a single coherent redistribution model that can be applied to both U-Zr and U-Pu-Zr fuel is required. Unfortunately, the phase complexity that results from introduction of plutonium has hampered the application of the thermochemistry-informed model by Hirschhorn et al. [190], despite the advantageous lower-length-scale-informed handling of zirconium redistribution afforded through a Computer Coupling of Phase Diagrams and Thermochemistry (CALPHAD) type materials analysis [196].

Perhaps the strongest case for an advanced constituent redistribution model is the potential to leverage phase-dependent properties to accurately represent the evolving microstructure of U-xPu-yZr during irradiation. Properties clearly vary by phase, as seen throughout many of the

models described in Section 4.2 . If either old experimental data can be reassessed or new data captured with phase dependence as a key parameter, a true mechanistic response of the fuel could be simulated.

Another key model absent from these simulations is the growth and impact of the FCCI that occurs at high doses [121, 197]. The weakening of the cladding that results from the wastage zone where FCCI occurs has a high impact on the transient response of the fuel system and is often the limiting factor in total fuel BU [198, 21]. Recently, LIFE-METAL correlations have been implemented into BISON and show promise in capturing an empirical FCCI growth rate [199, 200]. In addition, limited work has shown that lanthanide migration to the fuel-cladding interface is enabled by the interconnected porosity network [104, 201, 202]. In order to be fully useful as a mechanistic tool, FCCI requires extensive development of lower-length-scale simulations to get species behavior, cracking responses to predict FCCI growth locations, and thermochemical-based models to capture the interdiffusion of lanthanides into the cladding and iron into the fuel [106]. By leveraging the results from such simulations, a combined FCCI model would provide a truly predictive cladding response.

One of the most complicated models for any nuclear fuel is the swelling due to fission gas, along with its eventual release into the plenum. While the model described in Section 4.2.5.3 is simple in nature, the utilization of several calibrated parameters—in particular the anisotropic growth factor and retained gas parameter—provides a means to reproduce the expected fuel response as a function of BU. Unfortunately, such a model does not hold the same usefulness or applicability beyond the traditional EBR-II design and operational envelope, motivating the need for a model that is coupled to the fuel state variables, namely temperature and stress. Similar to FCCI, a model that captures a more mechanistic fuel response is under development in BISON [203] but has only been tested in a limited sense such that its ability to reproduce the expected fission gas release will be the focus of future work.

While an advanced high-temperature swelling model is well underway for incorporation into U-xPu-yZr simulations, BISON still lacks a mechanistic hot pressing and low-temperature fission gas swelling capability [204]. Such models require information from crystal-plasticity lower-length-scale simulations in order to mechanistically reproduce the fuel response in the low-temperature phase region. In addition, advanced visco-plastic methods implemented in MOOSE help capture the complex temperature and irradiation-dependent plastic response of the fuel [205, 185, 206].

The cladding strain response provides an excellent tool for quantitatively comparing BISON simulations to easily measured, nondestructive values. Consequently, the constituent model used to capture the cladding response to stress is essential. Developing a single model that captures cladding behavior under prototypical operation conditions is difficult given the limited data [207]. To that end, reduced-order models informed from lower-length-scale simulations could provide an excellent tool to more accurately calculate the cladding response [135, 132].

In order to truly assess the success of BISON as a tool to simulate U-xPu-yZr fuel, a database of assessments is required to fill out the operating envelope of the fuel system. Several scattered assessments exist that would benefit from adopting the baseline capabilities outlined in this paper [208, 37, 209, 210, 211]. This could be especially enlightening when comparing the fuel response between the EBR-II and FFTF fuel designs, which will naturally help separate the impact of temperature and fission rate [106]. This data has begun being collected into a single database, with a number of assessments already performed for rods other than those in X441 [143]. Only by increasing the total number of assessments in BISON, can BISON’s usefulness

be quantified and calibrated [212, 213, 214]. In particular, many of the parameters here would benefit from a formal uncertainty quantification and calibration treatment that could support advanced metallic fuel qualification.

5 CONCLUSIONS

This report documents experience with the U-Zr fuel system in fast reactors and presents the fuel qualification case for a data-supported fuel design and set of operating conditions. This is done by identifying as-fabricated conditions (e.g., dimensions, chemistry) and in-pile conditions (e.g., linear heat generation rates, BU, temperature) and AOOs. Within this safety case, we identified engineering and safety-significant parameters and phenomena present in the fuel system. Up to the proposed 10 at% BU limit, life-limiting and safety-related fuel behaviors are well known and predictable.

We identified the life-limiting phenomenon as FCCI, which leads to cladding and barrier degradation. This FCCI process is highly temperature sensitive and is represented in the safety case and operational envelope with an appropriate margin. In this report, we identified and discussed factors that influence temperature (e.g., porosity, thermal conductivity, fuel swelling) to ensure that the in-pile conditions remain favorable and known. As such, the FCCI phenomenon, while life-limiting, is acceptable within the operational bounds described in this report.

As such, this document serves as the beginning of the fuel qualification process for U-Zr for this particular use and safety case. Deviations from parameters, engineering or neutronic, we've identified here requires additional justification and discussion.

6 REFERENCES

[1] NRC. “Fuel Qualification for Advanced Reactors.” Report NUREG-2246. Nuclear Regulatory Commission, Mar. 2022.

[2] L. Walters. “Thirty years of fuels and materials information from EBR-II.” In: *J. Nucl. Mat.* 270.1-2 (1999): pp. 39–48. ISSN: 0022-3115. https://doi.org/10.1016/S0022-3115(98)00760-0. URL: https://www.sciencedirect.com/science/article/pii/S0022311598007600.

[3] Douglas C. Crawford, et al. “An approach to fuel development and qualification.” In: *Journal of Nuclear Materials* 371.1-3 (2007): pp. 232–242. ISSN: 00223115. https://doi.org/10.1016/j.jnucmat.2007.05.029.

[4] W. J. Carmack, et al. “Metallic fuels for advanced reactors.” In: *Journal of Nuclear Materials* 392.2 (2009): pp. 139–150. ISSN: 0022-3115. https://doi.org/10.1016/J.JNUCMAT.2009.03.007. URL: https://www.sciencedirect.com/science/article/pii/S0022311509004103.

[5] Dawn E. Janney and Steven L. Hayes. “Experimentally Known Properties of U-10Zr Alloys: A Critical Review.” English. In: *Nuclear Technology* 203.2 (2018): pp. 109–128. ISSN: 00295450. https://doi.org/10.1080/00295450.2018.1435137.

[6] Walt Williams, et al. “Specification for the DISECT Fuel Fabrication.” In: Idaho National Laboratory SPC-2391 2 (2020).

[7] A. L. Pitner and R. B. Baker. “Metal Fuel Test Program in the FFTF.” In: *Journal of Nuclear Materials* 204 (Sept. 1993): pp. 124–130. ISSN: 00223115. https://doi.org/10.1016/0022-3115(93)90208-G.

[8] Douglas C. Crawford, Douglas L. Porter, and Steven L. Hayes. “Fuels for Sodium-Cooled Fast Reactors: US Perspective.” In: *Journal of Nuclear Materials* 371.1-3 (Sept. 2007): pp. 202–231. ISSN: 00223115. https://doi.org/10.1016/j.jnucmat.2007.05.010.

[9] Alvia E. Bridges, et al. “A Liquid-Metal Reactor Core Demonstration Experiment Using HT-9.” In: *Nuclear Technology* 102.3 (June 1993): pp. 353–366. ISSN: 0029-5450, 1943-7471. https://doi.org/10.13182/NT93-A17034.

[10] Christopher Matthews, et al. “Development and formulation of physics based metallic fuel models and comparison to integral irradiation data.” In: *Journal of Nuclear Materials* (Under Review) (2022).

[11] C. E. Lahm, et al. “Experience with advanced driver fuels in EBR-II.” In: *Journal of Nuclear Materials* (1993). ISSN: 00223115. https://doi.org/10.1016/0022-3115(93)90207-F.

[12] B. R. Seidel, L. C. Walters, and Y. I. Chang. “Advances in Metallic Nuclear Fuel.” In: *Jom* 39.4 (1987): pp. 10–13. ISSN: 10474838. https://doi.org/10.1007/BF03258852.

[13] C. W. Wilkes, D .B. Tracy, V. Griffiths, et al. “EBR-II fuel slug casting experience.” Report AL-IFR-73. Argonne National Lab.(ANL), Argonne, IL (United States), 1987.

[14] Alan Edward Waltar and Albert Barnett Reynolds. "Fast breeder reactors." Alan E. Waltar, 1981.

[15] A. L. Pitner and R. B. Baker. "Metal fuel test program in the FFTF." In: J*ournal of Nuclear Materials* 204.C (1993): pp. 124–130. ISSN: 00223115. https://doi.org/10.1016/0022-3115(93)90208-G.

[16] N. E. Dodds, D. L. Porter, et al. "EBR-II Production Fuel Slugs and Production Fuel Elements." In: Argonne National Laboratory Specification No. EI257-0005-ES-OO (1988).

[17] N. E. Dodds, H. C Tsai, et al. "FFTF Fuel Element Fabrication Requirements." In: Argonne National Laboratory Specification No. FOOOI-0035-DS (1986).

[18] Alvia E. Bridges, et al. "Liquid metal reactor core demonstration experiment using HT-9." In: *Nuclear Technology* 102.3 (1993): pp. 353–366. ISSN: 00295450. https://doi.org/10.13182/NT93-A17034.

[19] R. G. Pahl, C. E. Lahm, and S. L. Hayes. "Performance of HT9 clad metallic fuel at high temperature." In: *Journal of Nuclear Materials* (1993). ISSN: 00223115. https://doi.org/10.1016/0022-3115(93)90210-P.

[20] Kyle M. Paaren, et al. "Cladding profilometry analysis of experimental breeder Reactor-II metallic fuel pins with ht9, d9, and ss316 cladding." In: *Energies* 14.2 (2021). ISSN: 19961073. https://doi.org/10.3390/en14020515.

[21] G. L. Hofman, L. C. Walters, and T. H. Bauer. "Metallic fast reactor fuels." In: *Progress in Nuclear Energy* 31 (Jan. 1997): pp. 83–110.

[22] Gerard L. Hofman, et al. "Swelling behavior of U-Pu-Zr fuel." In: *Metallurgical Transactions* A 21.2 (Feb. 1990): pp. 517–528.

[23] J. Rest. "Kinetics of fission-gas-bubble-nucleated void swelling of the alpha-uranium phase of irradiated U-Zr and U-Pu-Zr fuel." In: *Journal of Nuclear Materials* 207 (1993): pp. 192–204. ISSN: 00223115. https://doi.org/10.1016/0022-3115(93)90261-V.

[24] Gerard L. Hofman, et al. "Swelling behavior of U-Pu-Zr fuel." In: *Metallurgical Transactions* A 21.2 (1990): pp. 517–528. ISSN: 0360-2133. https://doi.org/10.1007/BF02671924. URL: http://link.springer.com/10.1007/BF02671924.

[25] J. M. Kramer, et al. "Modeling the behavior of metallic fast reactor fuels during extended transients." In: *Journal of Nuclear Materials* 204 (1993): pp. 203–211. ISSN: 00223115. https://doi.org/10.1016/0022-3115(93)90218-N.

[26] J. Galloway, et al. "Modeling constituent redistribution in U–Pu–Zr metallic fuel using the advanced fuel performance code BISON." In: *Nuclear Engineering and Design* 286 (2015): pp. 1–17. ISSN: 00295493. https://doi.org/10.1016/j.nucengdes.2015.01.014. URL: https://www.sciencedirect.com/science/article/pii/S0029549315000552.

[27] W. J. Carmack, et al. “Metallography and fuel cladding chemical interaction in fast flux test facility irradiated metallic U-10Zr MFF-3 and MFF-5 fuel pins.” In: *Journal of Nuclear Materials* 473 (2016): pp. 167–177. ISSN: 00223115. https://doi.org/10.1016/j.jnucmat.2016.02.019.

[28] Jason M. Harp, et al. “Scanning electron microscopy examination of a Fast Flux Test Facility irradiated U-10Zr fuel cross section clad with HT-9.” In: *Journal of Nuclear Materials* 494 (2017): pp. 227–239. ISSN: 00223115. https://doi.org/1016/j.jnucmat.2017.07.040.

[29] J. Rest. “Modeling of fission-gas-induced swelling of nuclear fuels.” In: *Comprehensive Nuclear Materials*. 2012. ISBN: 9780080560335. https://doi.org/10.1016/B978-0-08-056033-5.00072-0.

[30] Ki Hwan Kim, et al. “Microstructural characterization of U-Zr alloy fuel slugs for sodium-cooled fast reactor.” In: *Surface and Interface Analysis*. 2012, pp. 1515–1518. https://doi.org/10.1002/sia.4989.

[31] C. M. Walters, G. H. Golden, and N. J. Olson. “U-Pu-Zr Metal Alloy: A Potential Fuel For LMFBR’S.” In: Argonne National Laboratory, ANL-76-28 (1975).

[32] Takanari Ogata, Yeon Soo Kim, and A. M. Yacout. “Metal Fuel Performance Modeling and Simulation.” In: *Comprehensive Nuclear Materials*. 2012, pp. 713–753. ISBN: 9780080560335. https://doi.org/10.1016/B978-0-08-056033-5.00075-6.

[33] R. G. Pahl, et al. “Experimental studies of U-Pu-Zr fast reactor fuel pins in the experimental breeder reactor-II.” In: *Metallurgical Transactions* A 21.7 (1990): pp. 1863–1870. ISSN: 0360-2133. https://doi.org/10.1007/BF02647233. URL: http://link.springer.com/10.1007/BF02647233.

[34] Andrei V. Gribok, et al. “Automatic information extraction from neutron radiography imaging to estimate axial fuel expansion in EBR-II.” In: *Journal of Nuclear Materials* 557 (2021): p. 153250. ISSN: 00223115. https://doi.org/10.1016/j.jnucmat.2021.153250.

[35] D. L. Porter, et al. “Performance of low smeared density sodium-cooled fast reactor metal fuel.” In: *Journal of Nuclear Materials* 465 (2015): pp. 464–470. ISSN: 00223115. http://dx.doi.org/10.1016/j.jnucmat.2015.06.014.

[36] D. L. Porter and D. C. Crawford. “Fuel Performance Design Basis for the Versatile Test Reactor.” In: *Nuclear Science and Engineering* 00.00 (2022): pp. 1–13. ISSN: 1943748X. https://doi.org/10.1080/00295639.2021.2009983.

[37] Kyle M. Paaren, et al. “Cladding Profilometry Analysis of Experimental Breeder Reactor-II Metallic Fuel Pins with HT9, D9, and SS316 Cladding.” In: *Energies* 14 (2021): p. 515.

[38] A. M. Yacout, et al. “FIPD: EBR-II Fuels Irradiation & Physics Database.” In: Argonne National Laboratory ANL-ART-124 (2017).

[39] K. M. Paaren, et al. “Initial demonstration of Automated fuel performance modeling with 1,977 EBR-II metallic fuel pins using BISON code with FIPD and IMIS databases.” In: *J. Nucl. Mater.* (2020).

[40] T. Ogawa, T. Iwai, and M. Kurata. “Demixing of U-Zr alloys under a thermal gradient.” In: J*ournal of the Less Common Metals* 175.1 (1991): pp. 59–69. ISSN: 00225088. https://doi.org/10.1016/0022-5088(91)90349-9.

[41] Gerard L. Hofman, S .L. Hayes, and M. C. Petri. “Temperature gradient driven constituent redistribution in U-Zr alloys.” In: *Journal of Nuclear Materials* 227.3 (1996): pp. 277–286. ISSN: 0022-3115. https://doi.org/10.1016/0022-3115(95)00129-8. URL: https://www.sciencedirect.com/science/article/pii/0022311595001298.

[42] R. R. Mohanty, et al. “Thermotransport in γ(bcc) U-Zr alloys: A phase-field model study.” In: *Journal of Nuclear Materials* 414 (2011): pp. 211–216. ISSN: 00223115. https://doi.org/10.1016/j.jnucmat.2011.03.028.

[43] G. Ondracek and B. Schulz. “The porosity dependence of the thermal conductivity for nuclear fuels.” In: *Journal of Nuclear Materials* (1973). ISSN: 00223115. https://doi.org/10.1016/0022-3115(73)90039-1.

[44] Weiming Chen and Xian-Ming Bai. “Temperature and composition dependent thermal conductivity model for U-Zr alloys.” In: *Journal of Nuclear Materials* 507 (2018): pp. 360-370. ISSN: 00223115. https://doi.org/10.1016/j.jnucmat.2018.05.021. URL: https://www.sciencedirect.com/science/article/pii/S0022311518302885.

[45] M. C. Petri and M. A. Dayananda. “Vacancy wind contributions to intrinsic diffusion.” In: Philosophical Magazine A: *Physics of Condensed Matter, Structure, Defects and Mechanical Properties* 76.6 (1997): pp. 1169–1185. ISSN: 01418610. https://doi.org/10.1080/01418619708214221.

[46] R. I. Sheldon and D. E. Peterson. “The U-Zr (Uranium-Zirconium) system.” In: *Bulletin of Alloy Phase Diagrams* 10.2 (1989): pp. 165–171. ISSN: 01970216. https://doi.org/10.1007/BF02881432.

[47] Wei Xiong, et al. “Thermodynamic modeling of the U-Zr system - A revisit.” In: *Journal of Nuclear Materials* 443.1-3 (2013): pp. 331–341. ISSN: 0022-3115. https://doi.org/10.1016/J.JNUCMAT.2013.07.034. URL: https://www.sciencedirect.com/science/article/pii/S0022311513009227.

[48] A. A. Bauer, et al. “Constitution of Zirconium-Uranium Alloys Containing Oxygen or Nitrogen.” In: *Battelle Memorial Institute* BMI-1187 (1957).

[49] A. Karahan. “Development of a Thermal Conductivity Model for the Irradiated U-Pu-Zr Metallic Fuels.” In: T*ransactions of the American Nuclear Society* 117.1 (2017): pp. 563-566.

[50] T. H. Bauer. “A general analytical approach toward the thermal conductivity of porous media.” In: *International Journal of Heat and Mass Transfer* 36.17 (1993): pp. 4181–4191. ISSN: 00179310. https://doi.org/10.1016/0017- 9310(93)90080- P. URL: https://www.sciencedirect.com/science/article/pii/001793109390080P.

[51] Yoichi Takahashi, Michio Yamawaki, and Kazutaka Yamamoto. “Thermophysical properties of uranium-zirconium alloys.” In: *Journal of Nuclear Materials* 154.1 (1988): pp. 141–144. ISSN: 00223115. https://doi.org/10.1016/0022-3115(88)90127-4. URL: https://www.sciencedirect.com/science/article/pii/0022311588901274.

[52] J. K. Fink. “Thermophysical Properties of Uranium Dioxide.” In: *Journal of Nuclear Materials* 279 (2000): pp. 1–18. URL: https://www.sciencedirect.com/science/article/pii/S0022311599002731.

[53] J. D. Hales, et al. “BISON Theory Manual The Equations Behind Nuclear Fuel Analysis.” In: INL/EXT-13-29930 Rev. 3, Idaho National Laboratory, September (2016).

[54] Gerard L. Hofman. “Irradiation Behavior of Experimental Mark-II Experimental Breeder Reactor II Driver Fuel.” In: *Nuclear Technology* 47.1 (1980): pp. 7–22. ISSN: 0029-5450. https://doi.org/10.13182/NT80-A32408. URL: https://www.tandfonline.com/doi/full/10.13182/NT80-A32408.

[55] N. S. Cannon, F. H. Huang, and M. L. Hamilton. “Simulated transient behavior of HT9 cladding.” In: (No. WHC-SA-0127; CONF-880613-23). Westinghouse Hanford Co., Richland, WA (USA) (1988).

[56] Gerard L. Hofman, L. C. Leon, C Walters, and T. H. Bauer. “Metallic fast reactor fuels.” In: *Progress in Nuclear Energy* 31.1 (1997): pp. 83–110. https://doi.org/10.1016/0149-1970(96)00005-4.

[57] Daniel M. Wachs, Luca Capriotti, and Douglas Porter. “Behavior of metallic fast reactor fuels during an overpower transient.” In: *Journal of Nuclear Materials* 557 (2021): p. 153304. ISSN: 0022-3115.

[58] L. Walters, et al. “Sodium Fast Reactor Fuels and Materials: Research Needs.” Report. Sandia National Lab.(SNL-NM), Albuquerque, NM (United States), 2012.

[59] Jake Hirschhorn, Ryan Sweet, and Jeffrey Powers. “Metallic Fuel Performance Code Requirements for the Versatile Test Reactor Project. Report.” Oak Ridge National Lab.(ORNL), Oak Ridge, TN (United States), 2021.

[60] Y. Y. Liu, et al. “Behavior of EBR-II Mk-V-type fuel elements in simulated loss-of-flow tests.” In: *Journal of Nuclear Materials* 204 (1993): pp. 194–202. ISSN: 0022-3115.

[61] T. H. Bauer, G. R. Fenske, and J. M. Kramer.” Cladding failure margins for metallic fuel in the integral fast reactor.” Tech. rep. 1987.

[62] Taeil Kim, et al. “Experimental studies on eutectic formation between metallic fuel and HT-9M cladding in a single-pin core structure of a sodium-cooled fast reactor.” In: *Journal of Nuclear Materials* 505 (2018): pp. 105–118. ISSN: 0022-3115.

[63] A. B. Cohen, H. Tsai, and L. A. Neimark. “Fuel/cladding compatibility in U-19Pu-10Zr/HT9-clad fuel at elevated temperatures.” In: *Journal of Nuclear Materials* 204 (1993): pp. 244–251. ISSN: 0022-3115.

[64] William J. Carmack. “Temperature and burnup correlated FCCI in U-10Zr metallic fuel.” Tech. rep. 2012.

[65] T. Sofu. “Fast reactor fuels.” In: U.S. Nuclear Regulatory Commission (2019).

[66] Christopher Matthews, et al. “Fuel-cladding chemical interaction in U-Pu-Zr metallic fuels: A critical review.” In: *Nuclear Technology* 198.3 (2017): pp. 231–259. ISSN: 00295450. https://doi.org/10.1080/00295450.2017.1323535.

[67] Kinya Nakamura, et al. “Reactions of Uranium-Plutonium Alloys with Iron.” In: *Journal of Nuclear Science and Technology* 38.2 (Feb. 2001): pp. 112–119. ISSN: 0022-3131, 1881-1248. https://doi.org/10.1080/18811248.2001.9715013.

[68] Takanari Ogata, et al. “Reactions between U–Zr Alloys and Fe at 1003K.” In: *Journal of Nuclear Materials* 441.1-3 (Oct. 2013): pp. 579–582. ISSN: 00223115. https://doi.org/10.1016/j.jnucmat.2012.09.038.

[69] Kinya Nakamura, et al. “Reactions of U–Zr Alloy with Fe and Fe–Cr Alloy.” In: *Journal of Nuclear Materials* 275.3 (Nov. 1999): pp. 246–254. ISSN: 00223115. https://doi.org/10.1016/S0022-3115(99)00227-5.

[70] Takanari Ogata, et al. “Reactions between U–Zr Alloys and Fe at 923 K.” In: (1997): p. 5.

[71] D. D. Keiser and M. A. Dayananda. “Interdiffusion between U-Zr Fuelvs Selected Cladding Steels.” In: *Metallurgical and Materials Transactions* A 25.8 (Aug. 1994): pp. 1649–1653. ISSN: 1073-5623,1543-1940. https://doi.org/10.1007/BF02668530.

[72] Dennis D. Keiser and Mark C. Petri. “Interdiffusion Behavior in U-Pu-Zr Fuel versus Stainless Steel Couples.” In: *Journal of Nuclear Materials* 240.1 (Dec. 1996): pp. 51–61. ISSN: 00223115. https://doi.org/10.1016/S0022-3115(96)00476-X.

[73] Okenta Inagaki, Kinya Nakamura, and Takanari Ogata. “Progress in Understanding of Fuel-Cladding Chemical interaction in Metal Fuel.” In: (2013).

[74] June-Hyung Kim, et al. “Measurement of microstructure and eutectic penetration rate on irradiated metallic fuel after high-temperature heating test.” In: *Metals and Materials International* 23.3 (2017): pp. 504–511. ISSN: 2005-4149.

[75] Theodore H. Bauer, et al. “Behavior of modern metallic fuel in treat transient overpower tests.” In: *Nuclear technology* 92.3 (1990): pp. 325–352. ISSN: 0029-5450.

[76] Group Fast Reactor Working Group. “Nuclear Metal Fuel: Characteristics, Design, Manufacturing, Testing, and Operating History.” In: White Paper 18-01. 2018.

[77] D. D. Keiser. “Fuel-cladding interaction layers in irradiated U-ZR and U-PU-ZR fuel elements.” Tech. rep. 2006. https://doi.org/10.1016/B978-0-08-056033-5.00067-7.

[78] D. D. Keiser Jr. “Recent Progress in Metal Fuel–Cladding Interaction Research.” In: Reference Module in *Materials Science and Materials Engineering*, Elsevier (2016).

[79] Dennis D. Keiser Jr. and Dennis D. Keiser. “Fuel cladding chemical interaction in metallic sodium fast reactor fuels: A historical perspective.” In: *Journal of Nuclear Materials* 514 (2019): pp. 393–398. ISSN: 00223115. https://doi.org/10.1016/j.jnucmat.2018.09.045.

[80] B. D. Middleton, et al. “The Development of a Realistic Source Term for Sodium-Cooled Fast Reactors: Assessment of Current Status and Future Needs.” Tech. rep. SAND2011-3404. Sandia National Laboratory, 2011. URL: https://www.osti.gov/servlets/purl/1018468.

[81] D. Grabaskas, et al. “A Mechanistic Source Term Calculation for a Metal Fuel Sodium Fast Reactor.” In: *Proceedings of International Conference on Fast Reactors and Related Fuel Cycles: Next Generation Nuclear Systems for Sustainable Development,* Yekaterinburg, Russia Federation, 2017.

[82] L. Soffer, et al. “Accident Source Terms for Light-Water Nuclear Power Plants.” Tech. rep. NUREG 1465. U.S. Nuclear Regulatory Commission, Office of Nuclear Regulatory Research, 1995. URL: https://www.osti.gov/servlets/purl/1018468.

[83] D. Grabaskas, et al. “Regulatory Technology Development Plan Sodium Fast Reactor. Mechanistic Source Term Development.” Tech. rep. ANL-ART-3 79581. U.S. Nuclear Regulatory Commission, Office of Nuclear Regulatory Research, 2015. URL: https://doi.org/10.2172/1179443.

[84] A. J. Brunett, M. Bucknor, and D. Grabaskas. “Toward a Mechanistic Source Term in Advanced Reactors: Characterization of Radionuclide Transport and Retention in a Sodium Cooled Fast Reactor” Conf. Paper International Congress on Advances in Nuclear Power Plants.” In: Proc. of *International Congress on Advances in Nuclear Power Plants ICAPP 2016*. San Francisco, U.S.A., 2016.

[85] C. Jensen, D. Wachs, and H. Banu. “Fuel Safety Research Plan for Metallic Fast Reactor Fuels.” Tech. rep. INL/INT-18-51467, Idaho National Laboratory, 2018.

[86] L. E. Herranz, M. P. Kissane, and M. Garcıa. “Comparison of LWR and SFR in-containment source term: Similarities and differences.” In: *Progress in Nuclear Energy* 66 (2013): pp. 52–60. ISSN: 0149-1970. https://doi.org/10.1016/j.pnucene.2013.03.002. URL: https://www.sciencedirect.com/science/article/pii/S0149197013000474.

[87] Chan Bock Lee, Dae Ho Kim, and Youn Ho Jung. “Fission gas release and swelling model of metallic fast reactor fuel.” In: *Journal of Nuclear Materials* (2001). ISSN: 00223115. https://doi.org/10.1016/S0022-3115(00)00718-2.

[88] Bryan A. Chin, Robert J. Neuhold, and Jerry l. Straalsund. “Materials Development for Fast Breeder Reactor Cores.” In: *Nucl Technol* V 57.N 3 (1982): pp. 426–435. ISSN: 00295450. https://doi.org/10.13182/nt82-a26308.

[89] A. L. Pitner, S. L. Hecht, and R. G. Trenchard. “Nonswelling behavior of HT9 alloy irradiated to high exposure.” In: No. WHC-SA-1967; CONF-931160-32. Westinghouse Hanford Co. (1993).

[90] Y. Chang. “Technical rationale for metal fuel in fast reactors.” In: *Nuclear Engineering and Technology* 39.3 (2007). issn: 1738-5733.

[91] Hanchung Tsai. “Fuel/cladding compatibility in irradiated metallic fuel pins at elevated temperatures.” Tech. rep. CONF-900804–9. Argonne National Laboratory, Apr. 1990.

[92] Y. Y. Liu, et al. “Whole-Pin Furnace system: An experimental facility for studying irradiated fuel pin behavior under potential reactor accident conditions.” Tech. rep. CONF-900804-24. Argonne National Laboratory, May 1990.

[93] J. M. Kramer and T. H. Bauer. “Fuel damage during off-normal transients in metal-fueled fast reactors.” Tech. rep. CONF-900804–20. Argonne National Laboratory, Apr. 1990.

[94] Leon C. Walters, B. R. Seidel, and J. Howard Kittel. “Performance of Metallic Fuels and Blankets in Liquid-Metal Fast Breeder Reactors.” In: *Nuclear Technology* 65.2 (1984): pp. 179–231. ISSN: 0029-5450. https://doi.org/10.13182/NT84- A33408. URL: https://www.tandfonline.com/doi/full/10.13182/NT84-A33408.

[95] C. E. Lahm, et al. “EBR-II driver fuel qualification for loss-of-flow and loss-of-heat-sink tests without scram.” In: *Nuclear Engineering and Design* 101.1 (1987): pp. 25–34. https://doi.org/10.1016/0029-5493(87) 90147-6.

[96] Carolyn Tomchik and Aaron Oaks. “Status and Availability of OPTD, the Out-of-Pile Transient Database.” Tech. rep. ANL-ART-214. Argonne National Laboratory, 2020.

[97] A. B. Cohen, H. Tsai, and L. A. Neimark. “Fuel/cladding compatibility in U-19Pu-10Zr/HT9-clad fuel at elevated temperatures.” In: *Journal of Nuclear Materials* 204 (Sept. 1993): pp. 244–251.

[98] Matthew R. Denman. “Probabilistic transient analysis of fuel choices for sodium fast reactors.” PhD thesis. *Massachusetts Institute of Technology*, 2011.

[99] X. Y. Liu, D. A. Andersson, and B. P. Uberuaga. “First-principles DFT modeling of nuclear fuel materials.” In: *Journal of Materials Science* 47.21 (2012): pp. 7367–7384. https://doi.org/10.1007/s10853-012-6471-6.

[100] T. H. Bauer. “In-Pile Measurement of the Thermal Conductivity of Irradiated Metallic Fuel.” In: *Nuclear Technology* 110.3 (1995): pp. 1–15.

[101] G. L. Hofman, et al. “*Metallic fuels handbook*.” Tech. rep. Argonne National Laboratory (ANL), Argonne, IL (United States), Nov. 1985.

[102] Aydin Karahan and Nathan C. Andrews. “Extended fuel swelling models and ultra high burn-up fuel behavior of U–Pu–Zr metallic fuel using FEAST-METAL.” In: *Nuclear Engineering and Design* 258 (May 2013): pp. 26–34.

[103] D. L. Porter and Hanchung Tsai. “Full-length U-xPu-10Zr (x=0, 8, 19wt.%) fast reactor fuel test in FFTF.” In: *Journal of Nuclear Materials* 427.1-3 (Aug. 2012): pp. 46–57.

[104] Chao Jiang, et al. “Bulk and surface diffusion of neodymium in alpha-uranium: Ab initio calculations and kinetic Monte Carlo simulations.” In: *Journal of Nuclear Materials* 557 (Dec. 2021): p. 153307.

[105] R. D. Mariani, et al. “Lanthanides in metallic nuclear fuels: Their behavior and methods for their control.” In: *Journal of Nuclear Materials* 419 (Dec. 2011): pp. 263–271.

[106] Christopher Matthews, et al. “Fuel-Cladding Chemical Interaction in U-Pu-Zr Metallic Fuels: A Critical Review.” In: *Nuclear Technology* 198.3 (June 2017): pp. 231–259.

[107] D. D. Keiser Jr. “3.15 - Metal Fuel-Cladding Interaction.” In: *Comprehensive Nuclear Materials*. Ed. By Rudy J. M. Konings. *Elsevier*, Feb. 2012, pp. 423–441.

[108] Walter James Williams. “The Crystallographic Evolution in the Uranium-Zirconium System.” Apr. 2022.

[109] T. Ogata, Yeon Soo Kim, and A. M. Yacout. “3.23 - Metal Fuel Performance Modeling and Simulation.” In: *Comprehensive Nuclear Materials*. Ed. by Rudy J, M, Konings. *Elsevier*, Feb. 2012, pp. 713–753.

[110] A. M. Yacout and M. C. Billone. “Current Status of the LIFE Fast Reactors Fuel Performance Codes.” In: *International Conference on Fast Reactors and Related Fuel Cycles Safe Technologies and Sustainable Scenarios FR*. Argonne National Laboratory. Mar. 2013.

[111] Y. Tsuboi, et al. “Design of the 4S Reactor.” In: *Nuclear Technology 178* (May 2012): pp. 201–217.

[112] G. L. Beausoleil, et al. “*Integrating Advanced Modeling and Accelerated Testing for a Modernized Fuel Qualification Paradigm*.” In: *Nuclear Technology* 207.10 (Aug. 2021): pp. 1491–1510.

[113] Richard C. Martineau. “The MOOSE Multiphysics Computational Framework for Nuclear Power Applications: A Special Issue of Nuclear Technology.” In: *Nuclear Technology* 207.7 (Sept. 2021): pp. 3–8.

[114] Romain Perriot, et al. “Atomistic modeling of out-of-pile xenon diffusion by vacancy clusters in UO2.” In: *Journal of Nuclear Materials* 520 (July 2019): pp. 96–109.

[115] D. A. Andersson, et al. “Density functional theory calculations of the thermodynamic and kinetic properties of point defects in -U.” In: *Journal of Nuclear Materials* 557 (Dec. 2021): p. 153238.

[116] Michael R. Tonks, et al. “Multiscale development of a fission gas thermal conductivity model: Coupling atomic, meso and continuum level simulations.” In: J*ournal of Nuclear Materials* 440.1-3 (Sept. 2013): pp. 193–200.

[117] Michael R. Tonks, et al. “Mechanistic materials modeling for nuclear fuel performance.” In: *Annals of Nuclear Energy* 105 (July 2017): pp. 11–24.

[118] Michael W.D. Cooper, et al. “Fission gas diffusion and release for CrO-doped UO: From the atomic to the engineering scale.” In: *Journal of Nuclear Materials* 545 (Mar. 2021): p. 152590.

[119] K. Govers, et al. “Molecular dynamics study of Xe bubble re-solution in UO2.” In: *Journal of Nuclear Materials* 420.1-3 (Jan. 2012): pp. 282–290.

[120] David C. Parfitt and Robin W. Grimes. “Predicting the probability for fission gas resolution into uranium dioxide.” In: *Journal of Nuclear Materials* 392.1 (July 2009): pp. 28–34.

[121] Christopher Matthews, Daniel Schwen, and Andrew C Klein. “Radiation re-solution of fission gas in non-oxide nuclear fuel.” In: *Journal of Nuclear Materials* 457.C (Feb. 2015): pp. 273–278.

[122] M. W. D. Cooper, et al. “Simulation of radiation driven fission gas diffusion in UO2, ThO2 and PuO2.” In: *Journal of Nuclear Materials* 481.C (Dec. 2016): pp. 125–133.

[123] Jonathan L. Wormald and Ayman I. Hawari. “Examination of the impact of electron-phonon coupling on fission enhanced diffusion in uranium dioxide using classical molecular dynamics.” In: *J. Mater. Res*., 30.9 (May 2015): pp. 1485–1494.

[124] D. Schwen, et al. “Molecular dynamics simulation of intragranular Xe bubble re-solution in UO2.” In: *Journal of Nuclear Materials* 392.1 (July 2009): pp. 35–39.

[125] R. A. Lebensohn and C. N. Tom´e. “A self-consistent anisotropic approach for the simulation of plastic deformation and texture development of polycrystals: Application to zirconium alloys.” In: *Acta Metallurgica et Materialia* 41.9 (Sept. 1993): pp. 2611–2624.

[126] Christopher Matthews, et al. “Cluster dynamics simulation of uranium self-diffusion during irradiation in UO2.” In: *Journal of Nuclear Materials* 527 (Dec. 2019), p. 151787.

[127] Christopher Matthews, et al. “Cluster dynamics simulation of xenon diffusion during irradiation in UO2.” In: *Journal of Nuclear Materials* 540 (Nov. 2020): p. 152326.

[128] M. W. D. Cooper, et al. “Irradiation-enhanced diffusion and diffusion-limited creep in U3Si2.” In: *Journal of Nuclear Materials* 555 (Nov. 2021): p. 153129.

[129] K. A. Gamble, et al. “Improvement of the BISON modeling capabilities based on multiscale developments to modeling fission gas behavior.” In: *Journal of Nuclear Materials* 555 (Nov. 2021): p. 153097.

[130] Paul C. Millett, Michael Tonks, and S. B. Biner. “Mesoscale modeling of intergranular bubble percolation in nuclear fuels.” In: *Journal of Applied Physics* 111.8 (Apr. 2012): pp. 083511–8.

[131] Larry K. Aagesen, et al. “Phase-field simulations of fission gas bubbles in high burnup UO during steady-state and LOCA transient conditions.” In: *Journal of Nuclear Materials* 557 (Dec. 2021): p. 153267.

[132] W Wen et al. “Mechanism-based modeling of thermal and irradiation creep behavior: An application to ferritic/martensitic HT9 steel.” In: International Journal of Plasticity 126 (Mar. 2020): p. 102633.

[133] Michael R. Tonks, et al. “Mechanistic materials modeling for nuclear fuel performance.” In: *Annals of Nuclear Energy* 105 (July 2017): pp. 11–24.

[134] Aaron E. Tallman, et al. “Data-Driven Constitutive Model for the Inelastic Response of Metals: Application to 316H Steel.” In: *Integrating Materials and Manufacturing Innovation* 9.4 (Oct. 2020): pp. 339–357.

[135] Aaron E. Tallman, et al. “Surrogate Modeling of Viscoplasticity in Steels: Application to Thermal, Irradiation Creep and Transient Loading in HT-9 Cladding.” In: *JOM* 73.1 (Oct. 2020): pp. 126–137.

[136] W. Wen, et al. “A Physics-Based Crystallographic Modeling Framework for Describing the Thermal Creep Behavior of Fe-Cr Alloys.” In: *Metallurgical and Materials Transactions* A 48.5 (Feb. 2017): pp. 2603–2617.

[137] Cody J. Permann, et al. “MOOSE: Enabling massively parallel multiphysics simulation.” In: *SoftwareX* 11 (2020): p. 100430.

[138] Richard L. Williamson, et al. “BISON: A Flexible Code for Advanced Simulation of the Performance of Multiple Nuclear Fuel Forms.” In: *Nuclear Technology* 207.7 (Sept. 2021): pp. 954–980.

[139] R. L. Williamson, et al. “Multidimensional multiphysics simulation of nuclear fuel behavior.” In: *Journal of Nuclear Materials* 423 (Apr. 2012): pp. 149–163.

[140] J. Galloway, et al. “Modeling constituent redistribution in U–Pu–Zr metallic fuel using the advanced fuel performance code BISON.” In: *Nuclear Engineering and Design* 286 (2015): pp. 1–17.

[141] Yeon Soo Kim, et al. “Modeling of constituent redistribution in U–Pu–Zr metallic fuel.” In: *Journal of Nuclear Materials* 359.1-2 (Dec. 2006): pp. 17–28.

[142] Yeon Soo Kim, et al. “Constituent redistribution in U–Pu–Zr fuel during irradiation.” In: *Journal of Nuclear Materials* 327.1 (Apr. 2004): pp. 27–36.

[143] Abdellatif M Yacout, et al. “FIPD: The SFR metallic fuels irradiation & physics database.” In: *Nuclear Engineering and Design* 380 (Aug. 2021): p. 111225.

[144] Alan E Waltar and Albert B Reynolds. “Fast Breeder Reactors.” New York, USA: *Pergamon Press*, 1981.

[145] Argonne National Laboratory. “EBR-II: Sixteen Years Of Operation.” Tech. rep. Idaho Falls, ID: Argonne National Laboratory, May 1980.

[146] Dawn E. Janney and Steven L. Hayes. “Experimentally Known Properties of U-10Zr Alloys: A Critical Review.” In: *Nuclear Technology* 203.2 (July 2018): pp. 109–128.

[147] Dawn E. Janney, Steven L. Hayes, and Cynthia A. Adkins. “A Critical Review of the Experimentally Known Properties of U-Pu-Zr Alloys. Part 2: Thermal and Mechanical Properties.” In: *Nuclear Technology* 206.1 (Dec. 2019): pp. 1–22.

[148] Dawn E. Janney and Cynthia A. Papesch.” *FCRD Transmutation Fuels Handbook 2015*.” Tech. rep. INL/EXT-15-36520. Idaho National Laboratory, 2015.

[149] Shuxiang Zhou, et al. “Combined ab initio and empirical model of the thermal conductivity of uranium, uranium-zirconium, and uranium-molybdenum.” In: (Aug. 2018): pp. 1–21.

[150] Shiyi Wen, et al. “A new model to describe composition and temperature dependence of thermal conductivity for solution phases in binary alloys.” In: *Journal of Materials Science & Technology* 59 (Dec. 2020): pp. 72–82.

[151] Yeon Soo Kim, Tae Won Cho, and Dong-Seong Sohn. “Thermal conductivities of actinides (U, Pu, Np, Cm, Am) and uranium-alloys (U-Zr, U-Pu-Zr and U-Pu-TRU-Zr).” In: *Journal of Nuclear Materials* 445.1-3 (2014): pp. 272–280.

[152] W. Chen and X-M Bai. “Temperature and composition dependent thermal conductivity model for U-Zr alloys.” In: *Journal of Nuclear Materials* 507 (2018): pp. 360–370.

[153] Shuxiang Zhou, Yongfeng Zhang, and Dane Morgan. “An Ab-Initio Based Semi-Empirical Thermal Conductivity Model for Multiphase Uranium-Zirconium Alloys.” In: *Journal of Nuclear Materials* 553 (Sept. 2021): p. 153044. ISSN: 00223115. https://doi.org/10.1016/j.jnucmat.2021.153044.

[154] J. K. Fink and L. Leibowitz. “Thermal conductivity of zirconium.” In: *Journal of Nuclear Materials* 226.1-2 (Oct. 1995): pp. 44–50.

[155] Y. S. Touloukian, et al. “Thermophysical Properties of Matter - The TPRC Data Series. Volume 1. Thermal Conductivity - Metallic Elements and Alloys.” In: (1970).

[156] C. A. Alexander and Van E. Wood. “Thermal conductivity of plutonium above room temperature.” In: *Journal of Applied Physics* 103.6 (2008): pp. 063704–8.

[157] Santu Kaity, et al. “Microstructural and thermophysical properties of U-6 wt.alloy for fast reactor application.” In: *Journal of Nuclear Materials* 427.1-3 (Aug. 2012): pp. 1–11.

[158] Yoichi Takahashi, Michio Yamawaki, and Kazutaka Yamamoto. “Thermophysical properties of uranium-zirconium alloys.” In: *Journal of Nuclear Materials* 154.1 (1988), pp. 141–144.

[159] R. C. Westphal. “Thermal Conductivity of Reactor Fuel Element Materials.” Tech. rep. AECD-3864. Westinghouse Electric Corporation, June 1954.

[160] L. R. McCreight. “Thermal Conductivity Data for Some Nuclear Fuels.” Tech. rep. TID-10062. Knolls Atomic Power Laboratory, Oct. 1952.

[161] G. Bing, F. W. Fink, and H. B. Thompson. “The thermal and electrical conductivities of zirconium and its alloys.” Tech. rep. BMI-65. *Battelle Memorial Institute*, 1951.

[162] Argonne National Labortaory. “Reactor Development Program Progress Report, June 1966.” Tech. rep. ANL-7230. Argonne National Laboratory, June 1966.

[163] “Metallurgy Division Annual Progress Report for 1965.” (Oct. 1967).

[164] R. Boucher and P. Barthelemy. “Comparison of U-Pu-Mo, U-Pu-Nb, U-Pu-Ti and U-Pu-Zr alloys.” Tech. rep. CEA-R 2531. *CEA*, 1964.

[165] D. R. Harbur, J. W. Anderson, and W. J. Maraman. “Studies on the U-Pu-Zr Alloy System for Fast Breeder Reactor Applications.” Tech. rep. LA-4512. Los Alamos Scientific Laboratory, Aug. 1970.

[166] L. R. Kelman, et al. “Status of metallic plutonium fast power-breeder fuels.” In: *Third International Conference on Plutonium*. London, Nov. 1965, pp. 458–484.

[167] H. Savage. “The heat content and specific heat of some metallic fast-reactor fuels containing plutonium.” In: *Journal of Nuclear Materials* 25.3 (Mar. 1968): pp. 249–259.

[168] G. L. Hofman, et al. *Metallic Fuels Handbook*. Tech. rep. ANL-NSE-3. Argonne National Laboratory (ANL), Argonne, IL (United States), Apr. 2019.

[169] F. A. Rough. “An Evaluation of Data on Zirconium-Uranium Alloys.” Tech. rep. DMI-1030. *Battelle Memorial Institute*, Aug. 1955.

[170] T. Ogata. “3.01 - Metal Fuel.” In: *Comprehensive Nuclear Materials*. Ed. by Rudy J. M. Konings. *Elsevier*, Feb. 2012, pp. 1–40.

[171] Argonne National Laboratory. “Reactor Development Program Progress Report." Tech. rep. ANL-7105. Argonne National Laboratory, Sept. 1965.

[172] J. H. Kittel, et al. “Plutonium and plutonium alloys as nuclear fuel materials.” In: *Nuclear Engineering and Design* 15 (Jan. 1971): pp. 373–440.

[173] Takanari Ogata and Takeshi Yokoo. “Development and Validation of ALFUS: An Irradiation Behavior Analysis Code for Metallic Fast Reactor Fuels.” In: *Nuclear Technology* (1999). ISSN: 0029-5450. https://doi.org/10.13182/NT99-A3018.

[174] H. J. Matzke. “Science of advanced LMFBR fuels.” 1986.

[175] Pavel Medvedev. “Fuel Performance Modeling Results for Representative FCRD Irradiation Experiments: Projected Deformation in the Annular AFC-3A U-10Zr Fuel Pins and Comparison to Alternative Designs.” Tech. rep. INL/EXT-12-27183. Idaho National Laboratory, Idaho Falls, ID: Sept. 2012.

[176] Aydin Karahan and Jacopo Buongiorno. “A new code for predicting the thermo-mechanical and irradiation behavior of metallic fuels in sodium fast reactors.” In: *Journal of Nuclear Materials* 396 (Jan. 2010): pp. 283–293.

[177] Chan Bock Lee, Dae Ho Kim, and Youn Ho Jung. “Fission gas release and swelling model of metallic fast reactor fuel.” In: *Journal of Nuclear Materials* 288.1 (Jan. 2001): pp. 29–42.

[178] Di Yun, et al. “An initial assessment of a mechanistic model, GRASS-SST, in U-Pu-Zr metallic alloy fuel fission-gas behavior simulations.” In: *Journal of Nuclear Materials* 435.1-3 (Apr. 2013): pp. 153–163.

[179] D. R. Olander. “Fundamental aspects of nuclear reactor fuel elements.” Technical Information Center, Energy Research and Development Administration, 1976.

[180] Theodore H. Bauer and John W. Holland. “In-Pile Measurement of the Thermal Conductivity of Irradiated Metallic Fuel.” In: *Nuclear Technology* 110.3 (1995): pp. 407–421.

[181] Y. S. Touloukian, et al. “Thermophysical Properties of Matter: The TPRC Data Series, Vol. 2.” Thermal Expansion: *Metallic Elements and Alloys*. New York, 1970.

[182] H. A. Saller, R. F. Dickerson, and W. E. Murr. “Uranium Alloys for High-Temperature Application.” Tech. rep. BMI-1098. Divison of Technical Information Extension, U.S. Atomic Energy Commission, June 1956.

[183] F. G. Foote, H. H. Chiswik, and R. E. Macherey. “Annual Progress Report for 1965 Metallurgy Division.” Tech. rep. ANL-7155. Argonne National Laboratory, 1965.

[184] A. Needleman and J. R. Rice. “Plastic creep flow effects in the diffusive cavitation of grain boundaries.” In: *Acta Metallurgica* 28.10 (Oct. 1980): pp. 1315–1332.

[185] J. B. Leblond, G. Perrin, and P. Suquet. “Exact results and approximate models for porous viscoplastic solids.” In: *International Journal of Plasticity* 10.3 (Jan. 1994): pp. 213–235.

[186] S. M. McDeavitt and A. A. Solomon. “Hot-isostatic pressing of U-10Zr by a coupled grain boundary diffusion and creep cavitation mechanism.” In: *Journal of Nuclear Materials* 228 (1996): pp. 184–200.

[187] M. V. Speight and W. Beere. “Vacancy Potential and Void Growth on Grain Boundaries.” In: *Metal Science* 9 (1975): pp. 190–191.

[188] W. Beere and M. V. Speight. “Creep cavitation by vacancy diffusion in plastically deforming solid.” In: *Metal Science* 12 (1978): pp. 172–176.

[189] I. W. Chen and A. S. Argon. “Diffusive Growth of Grain-boundary Cavities.” In: *Acta Metallurgica* 29 (1981): pp. 1759–1768.

[190] Jacob Hirschhorn, Michael Tonks, and Christopher Matthews. “A CALPHAD-informed approach to modeling constituent redistribution in Zr-based metallic fuels using BISON.” In: *Journal of Nuclear Materials* 544 (2021): p. 152657.

[191] Yeon Soo Kim, G. L. Hofman, and A. M. Yacout. “Migration of minor actinides and lanthanides in fast reactor metallic fuel.” In: *Journal of Nuclear Materials* 392.2 (July 2009): pp. 164–170.

[192] G. Bozzolo, et al. “Lanthanides migration in U-Zr based nuclear fuels.” In: *Journal of Nuclear Materials* 407.3 (Dec. 2010): pp. 228–231.

[193] G. L. Hofman, S. L. Hayes, and M. C. Petri. “Temperature gradient driven constituent redistribution in U-Zr alloys.” In: J*ournal of Nuclear Materials* 227.3 (Jan. 1996): pp. 277–286.

[194] Y. H. Sohn, et al. “Analysis of constituent redistribution in the γ (bcc) U–Pu–Zr alloys under gradients of temperature and concentrations.” In: *Journal of Nuclear Materials* 279.2-3 (June 2000): pp. 317–329.

[195] Christopher Matthews, Garrison Stevens, and Cetin Unal. “Calibration of Zr Redistribution Models for Metallic Fuel in BISON.” In: *American Nuclear Society Annual Meeting*. Philadelphia, PA, June 2018, pp. 1343–1346.

[196] Nigel Saunders and A Peter Miodownik. “CALPHAD (calculation of phase diagrams): a comprehensive guide.” *Elsevier*, 1998.

[197] G. L. Hofman, et al. “Chemical interaction of metallic fuel with austenitic and ferritic stainless steel cladding.” In: *International Conference on Reliable Fuels for Liquid Metal Reactors*. Tucson, AZ, September 7-11, 1986.

[198] Daniel M. Wachs, Luca Capriotti, and Douglas Porter. “Behavior of metallic fast reactor fuels during an overpower transient.” In: *Journal of Nuclear Materials* 557 (Sept. 2021), p. 153304.

[199] Yinbin Miao, et al. “Metallic Fuel Cladding Degradation Model Development and Evaluation for BISON.” In: *Nuclear Engineering and Design*.

[200] A. M. Yacout and M. C. Billone. “Current Status of the LIFE Fast Reactors Fuel Performance Codes.” In: *International Conference on Fast Reactors and Related Fuel Cycles Safe Technologies and Sustainable Scenarios FR*. Argonne National Laboratory. 2013, pp. 1-10.

[201] C. Unal, et al. “A Potential Mechanism for Lanthanide Transport in Metallic Fuels.” In: *Transactions of the American Nuclear Society* 116 (June 2017): pp. 501–503.

[202] Xiang Li, et al. “Ab-initio molecular dynamics study of lanthanides in liquid sodium.” In: *Journal of Nuclear Materials* 484 (Feb. 2017): pp. 98–102.

[203] Christopher Matthews and Cetin Unal. “Initial implementation of a new Fission Gas Swelling and Release Algorithm for Metallic Nuclear Fuel into BISON.” Tech. rep. LA-UR-18-23733. Los Alamos National Laboratory, Apr. 2018.

[204] J. Rest. “Kinetics of fission-gas-bubble-nucleated void swelling of the alpha-uranium phase of irradiated U-Zr and U-Pu-Zr fuel.” In: *Journal of Nuclear Materials* 207 (1993): pp. 192–204.

[205] Christopher Matthews, et al. “Combined Visco-Plasticity and Swelling in Metallic Nuclear Fuel.” Tech. rep. LA-UR-19-25483. LANL, June 2019.

[206] A. L. Gurson. “Continuum Theory of Ductile Rupture by Void Nucleation and Growth: Part I—Yield Criteria and Flow Rules for Porous Ductile Media.” In: *Journal of Engineering Materials and Technology* 99.1 (1977): pp. 2–63.

[207] Ho Jim Ryu, et al. “Review of HT-9 Cladding Creep Correlations for Advanced Liquid Metal Fast Reactors.” In: (Apr. 2006): pp. 1–2.

[208] Kyle M. Paaren, et al. “Initial demonstration of automated fuel performance modeling with 1977 EBR-II metallic fuel pins using BISON code with FIPD and IMIS databases.” In: *Nuclear Engineering and Design* 382 (Oct. 2021): p. 111393.

[209] Kaylee M. Cunningham, Jeffrey J. Powers, and Robert Alexander Lefebvre. “Modeling the IFR-1 Experiment: A BISON Metallic Fuel Benchmark.” In: (July 2019): pp. 1–49.

[210] Jacob A. Hirschhorn, et al. “Metallic Fuel Performance Benchmarks for Versatile Test Reactor Applications.” In: *Nuclear Science and Engineering* 00.00 (Mar. 2022): pp. 1–25.

[211] I. Greenquist, et al. “Development of a U-19Pu-10Zr fuel performance benchmark case based on the IFR-1 experiment.” In: *Journal of Nuclear Materials* 553 (2021): p. 152997.

[212] C. Unal, et al. “Application of advanced validation concepts to oxide fuel performance codes: LIFE-4 fast-reactor and FRAPCON thermal-reactor fuel performance codes.” In: *Nuclear Engineering and Design* 263 (Oct. 2013): pp. 102–128.

[213] C. Unal, et al. “Improved best estimate plus uncertainty methodology, including advanced validation concepts, to license evolving nuclear reactors.” In: *Nuclear Engineering and Design* 241.5 (May 2011): pp. 1813–1833.

[214] Cetin Unal, Garrison Nicole Stevens, and Christopher Matthews. “Progressive Bayesian Calibration of the BISON Fuel Performance Capability.” In: *Top Fuel*. Prague, Czech Republic, Sept. 2018.

APPENDIX A
RETROSPECTIVE OF NUREG-2246 APPLICATION TO U-ZR

Companies looking to license reactors with materials that differ from the current U.S. fleet of light-water zirconium-clad ceramic fuel are emerging as part of the push toward a more responsible energy economy. As such, the Nuclear Regulatory Commission (NRC) was tasked with evaluating these new license applications and implemented NUREG-2246 to aid in the fuel-specific qualification. Idaho National Laboratory trialed the process outlined in NUREG-2246 on the uranium-zirconium (U-Zr) fuel system. This appendix documents notable comments on the process, including strengths, suggestions, and areas requiring additional discussion.

A.1 Comments on the Process of Applying the NUREG and Suggestions for Updates

Existing fuel assessment guidance exists for traditional light-water reactors; however, there is a likely large influx of proposals that will differ in material and design. As such, the NRC created NUREG-2246 to identify nuclear fuel qualification criteria and a useful assessment framework for advanced reactor designers. Idaho National Laboratory has trialed the NUREG-2246 process on the metallic uranium-zirconium (U-Zr) fuel system for fast reactors. This trial included reporting fuel design specification, safety criteria, and a proposed fuel performance operating envelope supported by experimental data and modeling and simulation. This brief appendix discusses notable findings from the process. The introduction of NUREG-2246 outlines the purpose, definitions, safety case, scope, and quality assurance to provide a fuel qualification assessment framework for advanced reactor designs. Within this section, “Safety Case” was the only potential concern. There is a footnote with additional information, it states that “Safety Case” is undefined but commonly refers to fission product retention. This vagueness leaves the entire scope up for debate between the licensee and reviewers. It may be prudent to create a formal definition or rubric for what needs must be met or at least rephrase in a more succinct manner combined with the “Scope” section (1.4). This combination, while trivial, would help potential licensees view goals defined in the report as steps for determining the overall safety case. The “Quality Assurance” (QA) subsection emphasizes that expectations exist for quality assurance programs yet also states that “this report does not explicitly describe quality assurance expectations.” Examples of prominent QA programs are in fact provided and Section 3 does include specific guidance and requirements. Including explicit QA criteria is impractical and must be approached on a case-by-case basis, but repeated phrasing of “qualification activities be controlled consistent with the fuel’s importance to safety” implies that a minimum requirement exists and can be described. We recommend either including these minimum requirements here or replacing the soft phrasing with a caveat that, for example, “QA programs are generally required, as outlined in Section 3 and data falling outside of a QA program may be accepted on a case-by-case basis.” The main point of this concern arises with Section 1.4 and Section 3 being contradictory if interpreted incorrectly. The background section of the report identifies regulatory requirements and outlines the remaining portions of the report. The needs and goals are well described. However, throughout the remainder of the document, the purpose is called into question. It is our understanding that the process trialing is focused on a specific fuel type rather than an entire reactor. As such, we have identified the following questions or talking points:

- This comment is generic to the regulatory basis but will use fission product release as an example. Fission product release occurs on multiple scales, from the fuel matrix, to the plenum, to the coolant, to the reactor building, to the site, and to the public. Each has a design barrier to minimize the final release and depends on designs other than the fuel

(e.g., coolant type, core design, and reactor vessel). The regulations in 10 CFR 50.34(a)(1)(ii)(D), 10 CFR 52.47(a)(2)(iv), and 10 CFR 52.79(a)(1)(vi) require an evaluation of a postulated fission product release, which is explicitly stated in this report. However, this trial is specific to a fuel system and may not be able to address these regulations in full. In Section 2, these regulations are for the entire reactor and may not be resolved on the fuel system level. As written, it is unclear if these regulations need to be met at this stage or if only a source term must be provided. Section G.2.2 discusses these radionuclide release limits, but without having the entire reactor considered, it makes more sense to provide a source term and dismiss these needs. As such, it is possible that NUREG-2246 would benefit by simply calling for the source term of the fuel system under the prescribed operating envelope. Similar findings exist for cladding degradation (barrier degradation), where without postulating the coolant compatibility and pressure, one cannot form a concise response. We assume that the regulatory points are here as they may be addressed on the scale of fuel, which also implies that some of them may be answered elsewhere. In summary, we suggest a brief discussion be added to Section 2 stating that while all points must be met, it can be determined to require core specifics as it is impractical to hypothesize how the fuel system will fare under all possible core designs or coolant types.

- Fuel fabrication requirements elicit a similar vagueness under the assumption that the report shall focus on a fuel system alone. For example, texturing in U-Zr extruded fuel does impact fuel swelling, particularly fuel elongation. This elongation impacts reactivity but can be readily accounted for in the core design. While this seems like a simple process to address by discussing fuel texturing, fabrication techniques and dimensions must be known to quantify the level of importance. This seemingly leaves two options. One, define the fuel geometry and fabrication process. Two, identify only the phenomenon. Option one is unrealistic as defining the fuel geometry subsequently limits core design and thus provides little benefit for those diverging into novel areas. However, option two begs the question as to whether it is possible to identify all phenomena relying on the fuel fabrication process for all hypothetical reactors that may use it. In essence, it is unclear where the line could be drawn between generic fuel qualification and core design implications.
- Of the goals, G.2.3 (specifically G.2.3.2) seems unachievable in this venue as safe shutdown and control element insertion is reactor specific. Features such as fuel swelling, for example, may be known to any extent and favorable for most, but a core may still be designed such that the swelling is prohibitive. Moreover, reactors may or may not use control rods (e.g., drums) that are not impacted by fuel swelling. We believe the burden of assuring negative reactivity insertion should remain a reactor-specific requirement. Moreover, things like thermal conductivity or thermal expansion may influence the safe shutdown criteria and be favorable for one design and not another, leading to the next point.
- NUREG-2246 is clear and relatively concise as to what needs addressing. However, a layout for addressing these areas is less intuitive as many points are cyclical or redundant, requiring the licensee to pose a layout and determine if and how each point needs addressing. This may hinder NRC reviews as more license requests are generated. Having a layout that can be followed one to one in a response may prove valuable to the NRC. However, the burden of meeting the regulatory needs is on the licensee, and it may be inappropriate to overdefine a process as the licensee may be aware of new phenomena.

A.2 Comments Specific to U-Zr Fuel

Uranium-zirconium (U-Zr) was trialed through the NUREG-2246 process. This section outlines areas that may require additional coverage, research, and testing. These are not absolutes and may be resolved in various manners.

The primary concern for the U-Zr safety case arises when discussing transients, be it anticipated operation occurrences, design-basis accidents, or beyond-design-basis accidents. With the current level of transient testing, it is likely that the margins of safety are unnecessarily large. This stems from lack of currently available transient testing data. We recommend there be a table, graphic, or discussion of operating ranges showing allowable times at power and temperature for off-normal conditions. This task was not able to be populated with certainty with the current available data. While the U-Zr system is relatively simple to defend, having transient test data to incorporate will drastically simplify the process and establish better safety margins, limits, and ultimate competitiveness as a nuclear fuel. Steady-state operation of U-Zr is a more straightforward case to defend with large amounts of available data up to, and in some cases beyond, 10 at% burnup (BU). However, both steady-state and off-normal behaviors can benefit from the following areas being expanded upon through testing, analysis, or modeling:

- Total radial strain limits are typically adopted in a conservative manner following the methodology chosen for EBR-II Mark-V driver fuel or FFTF fuel as only limited data is available for modern fuel designs that have been “run to breach.” It is possible that the typically posed 1% peak cladding strain limit be required with available data, whereas the joint modeling and experiment effort imply that this value can be increased to 2–3%. This is not only more favorable from an operation standpoint but also serves to illustrate the robust nature of U-Zr and HT9 fuel systems. Additional work, likely a combination of modeling and experimentation, would likely be needed to increase the strain limits above 1%. This is less valuable for steady-state operation below 10 at% BU but becomes imperative to transient limits and increasing the BU ceiling above 10 at%.
- Along similar lines, plenum pressure limits for specific cladding designs should be defined; alternatively, cladding stress limits for non-specific dimensions of a specific cladding material could be defined. While little experimental data is available from breached systems, it is possible to calculate estimated fuel rod pressures in test rods. This, again, helps support the safety case under transient conditions. It also aids in the description of the fuel system and fabrication requirements. Understanding the pressures associated with these different systems may allow for novel designs or improved safety.
- A primary concern for any fuel system is to maintain coolability. The report, as it stands, addresses coolability during normal operations (and possibly during anticipated operational occurrences). However, it does not address coolability issues during transients. It would be beneficial, and possibly required, to expand upon the transient response from this respect, addressing behaviors such as cladding dilation and impact on coolant flow resistance and fuel or debris ejection from breached fuel rods and whether coolant channels might credibly be blocked or flow impeded.
- Similarly, fission product retention is a primary concern in any fuel system, particularly in cladding breach scenarios. This process would be aided by identifying any “run beyond cladding breach” tests, or post-irradiation fission gas analysis tests, to inform the level of fission product releases to the coolant under accident scenarios.
- It is unclear whether a fabrication process must be defined at this stage or if rigid geometries must be identified. This needs to be addressed during review. Should either be required, the report needs to be updated to include specific parameters, rather than

historically observed ranges (e.g., column length, pin width, cladding thickness). The applicant could provide details on how important fuel attributes would be controlled using a process specification, using a product specification, or some combination of both.

- U-Zr licensing may expand into novel geometries and conditions (power and BU). An additional section may be added to the report in an effort to identify the main concerns or areas where phenomena may be influence or changed.
- The fuel-cladding chemical interaction is the current life-limiting phenomenon in the U-Zr system. This is primarily due to the formation of a lower-melting-point (eutectic-like) phase, cladding wastage, and embrittlement of the cladding. While the report is fairly inclusive in discussing the fuel-cladding chemical interaction, it becomes convoluted discussing the various eutectics among the fuel constituents (U rich, Fe rich, lanthanide bearing), making it difficult to discern which compositions might form and at which local fuel temperatures. Again, this is more trivial for steady-state operation but becomes a concern for transients, leading back to the aforementioned point of outlining allowable times at power and temperature for off-normal conditions.

NRC FORM 335
(12-2010)
NRCMD 3.7

U.S. NUCLEAR REGULATORY COMMISSION

BIBLIOGRAPHIC DATA SHEET

(See instructions on the reverse)

1. REPORT NUMBER
(Assigned by NRC, Add Vol., Supp., Rev., and Addendum Numbers, if any.)

NUREG/CR-7305

2. TITLE AND SUBTITLE

Metal Fuel Qualification

Fuel Assessment Using NRC NUREG-2246, “Fuel Qualification for Advanced Reactors”

3. DATE REPORT PUBLISHED

MONTH	YEAR
August	2023

4. FIN OR GRANT NUMBER

5. AUTHOR(S)

W. Williams (1), C. Matthews (2), Y. Miao (3), F. Di Lemma (1), L. Capriotti (1), Y. Wang (1), C. Jensen (1), D. Keiser (1), C. Adkins (1), D. Crawford (1), S. Novascone (1), D. Wachs (1)

6. TYPE OF REPORT

Technical

7. PERIOD COVERED (Inclusive Dates)

8. PERFORMING ORGANIZATION - NAME AND ADDRESS (If NRC, provide Division, Office or Region, U. S. Nuclear Regulatory Commission, and mailing address; if contractor, provide name and mailing address.)

1. Idaho National Laboratory, Idaho Falls, ID 83415
2. Los Alamos National Laboratory, Los Alamos, NM 87545
3. Argonne National Laboratory, Argonne, IL 60439

9. SPONSORING ORGANIZATION - NAME AND ADDRESS (If NRC, type "Same as above", if contractor, provide NRC Division, Office or Region, U. S. Nuclear Regulatory Commission, and mailing address.)

Division of Systems Analysis
Office of Nuclear Regulatory Research
U.S. Nuclear Regulatory Commission
Washington, D.C. 20555-0001

10. SUPPLEMENTARY NOTES

First initial. Last name, or other notes as needed

11. ABSTRACT (200 words or less)

Companies looking to license reactors with different materials than the current U.S. fleet of light-water zirconium-clad ceramic fuel are emerging as part of the push toward a more responsible energy economy. As such, the Nuclear Regulatory Commission is tasked with evaluating these new license applications. This report documents the current state of available experiment measurements, simulation capability, and historic knowledge and lessons learned required for evaluating sodium-cooled fast-spectrum metallic fuel, specially U-10wt%Zr, up to 10at% burnup.

12. KEY WORDS/DESCRIPTORS (List words or phrases that will assist researchers in locating the report.)

Metallic fuel qualification, application of NUREG-2246

13. AVAILABILITY STATEMENT

unlimited

14. SECURITY CLASSIFICATION

(This Page)
unclassified

(This Report)
unclassified

15. NUMBER OF PAGES

16. PRICE

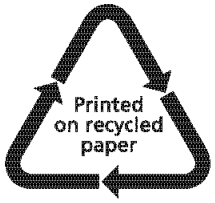

Federal Recycling Program

UNITED STATES
NUCLEAR REGULATORY COMMISSION
WASHINGTON, DC 20555-0001

OFFICIAL BUSINESS